

SYMMETRY LOWERING IN CRYSTALLINE SOLID SOLUTIONS.

A STUDY OF CINNAMAMIDE-THIENYLACRYLAMIDE BY X-RAY AND NEUTRON DIFFRACTION AND SOLID-STATE PHOTOCHEMISTRY

L.J.W. Shimon[‡], M. Vaidat[†], Y. Weissinger-Lewin^f, F. Frolow[†],
M. Lahav[†], L. Leiserowitz[†] and R.K. McMullan^f

RECEIVED

APR 07 1993

OSTI

Abstract

Principles are outlined for symmetry lowering of a mixed crystal composed of host and tailor-made additive molecules, based on selective occlusion of the latter through a subset of surface sites of the growing crystal, the symmetry of the surface generally being lower than that of the bulk. A survey is given of the various methods and approaches used to detect the reduction in symmetry. These include changes in crystal morphology, detection of enantiomeric segregation of chiral additives in "centrosymmetric" crystals, generation of second harmonic optical signals, optical birefringence, asymmetric photoreactions in the crystalline state and X-ray and neutron diffraction. The latter two methods are applied to mixed crystals of cinnamamide (host) and thienylacrylamide (additive). The diffraction analysis demonstrated that the mixed crystals are composed of six sectors of reduced symmetry, from monoclinic centrosymmetric $P2_1/c$ to triclinic $P1$ in four sectors and possibly Pc in the remaining two. The X-ray diffraction data were not sufficiently accurate to permit assignment of the absolute structures of the $P1$ sectors with the use of anomalous X-ray scattering. Thus, by this method one could not ascertain the absolute orientation of the guest molecules on the surface sites through which they were selectively occluded. This ambiguity was resolved by assignment of the absolute configuration of the chiral heterophotodimers, between host and guest, in enantiomeric excess in the $P1$ sectors, after irradiation with UV light. These results lead to the definite conclusion that the selective occlusion of thienylacrylamide arises from a replacement of attractive C-H $\cdots\pi$ (electron) interactions between host molecules by a repulsive sulfur (lone pair electron) $\cdots\pi$ (electron) interactions between guest and host at the crystal surfaces.

[‡] Present address; Department of Biochemistry and Molecular Biology, Harvard University, Cambridge, Mass. 02138

[†] Department of Materials and Interfaces, Weizmann Institute of Science, Rehovot 76100, Israel

^f Department of Chemistry, Brookhaven National Laboratory, Upton, NY 11973

MASTER
DISTRIBUTION OF THIS DOCUMENT IS UNLIMITED

Introduction

Principles of reduction in symmetry.

Recently we reported changes in crystal habit and composition during crystallization caused by the presence in solution of minor amounts (1-10%) of an additive with molecular structure similar to that of the host, but sufficiently different that only minute (up to 1%) amounts thereof were eventually occluded into the crystal¹⁻⁹. We could infer that the additive may be adsorbed only at the surface sites on those faces such that the part of the adsorbate that differs from the host emerges from the surface. Once adsorbed the additive inhibits the regular deposition of oncoming molecular layers leading to morphological changes as illustrated in scheme 1. The change is not only of a morphological nature, but may also be structural. For example, in view of selective adsorption and occlusion through a subset of crystal faces the additives will be anisotropically distributed within the crystal, leading to a mixed crystal of sectors coherently compounded together. Furthermore, since the point symmetries of the crystal faces are generally lower than that of the bulk, the additive may be occluded through a subset of surface sites on the preferred faces and so would occupy a subset of all the symmetry-related sites in the crystal leading to a reduction in crystal symmetry⁶⁻¹³.

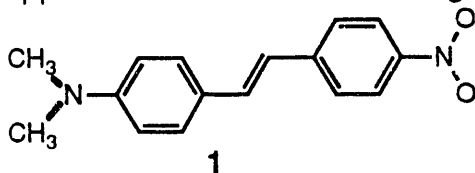
We shall illustrate the concept of reduction in crystal symmetry upon selective occlusion through an example of a schematic molecular arrangement in a motif of point group $2/m$ ¹⁴.

The packing arrangement in scheme 2 exhibits space symmetry $P2_1/c$. In this arrangement the open figures are related to the striped ones by twofold screw rotation, to the grey figures by glide symmetry and to the dashed ones by centers of inversion. Note the corresponding operations of the $2/m$ point symmetry. The crystal is delineated by three different sets of symmetry related faces, the two top and bottom $\{010\}$ faces, the four diagonal $\{011\}$ faces and the two opposite $\{001\}$ side faces. One can easily see in scheme 3 that an additive molecule, *in dark*, bearing an appropriately modified group will be able to substitute for one of the four different substrate molecules at each of the four diagonal $\{011\}$ faces. Occlusion of additive through the four diagonal faces will lead to a crystal composed of four sectors (scheme 3). The symmetry in each sector will be $P1$ in accordance with the surface symmetry of $p1$ of each of the four symmetry-related diagonal faces. Moreover the four sectors are related by the overall point

symmetry $2/m$ of the pure crystal. This result is in keeping with Curie's law¹⁵, which states that the *overall* symmetry of a system cannot be reduced unless outside asymmetric forces have been applied to the system.

Different methods for detection of symmetry lowering.

The reduction in symmetry of crystals was demonstrated by different methods on a variety of systems. One method, albeit far from definitive, involved change in morphology. This change indicated that the additive was preferentially bound to a subset of crystal faces, but only suggested that the additive was preferentially absorbed at a subset of symmetry-related sites on those faces, which would lead to a reduction in crystal symmetry upon eventual occlusion. A more conclusive method involved detection by HPLC of enantiomeric segregation of chiral additives occluded in "centrosymmetric" crystals. For example when the α -form of glycine, which in pure form is centrosymmetric monoclinic, is grown in an aqueous solution containing a racemic mixture of α -amino acids, the latter segregate into enantiomeric islands at opposite halves within the crystal along its symmetry axis. This separation into enantiomeric territories is a consequence of the chiral-selective adsorption and occlusion of the additives through the opposite enantiotopic (namely, of opposite chirality) faces of the crystal^{6,7,13}. Such enantiomeric segregation leading to a loss of crystallographic center of inversion was also observed in the host-guest systems of (R,S) serine-(R,S) threonine⁸ and glycylglycine-glycyl-(R,S)-leucine⁹. A loss of a crystallographic inversion symmetry was also detected by generation of a second harmonic optical signal, which is a fingerprint of an acentric crystal. The method is easily applicable if either the host or guest molecule has a large hyperpolarizability.



Thus second harmonic generation was detected in single crystals of α -glycine grown in the presence of the p-nitrophenyllysine and single crystals of 1 grown in presence of the dinitro derivative¹⁶. Note here that whereas the *molecular* structure of the host is non centrosymmetric, that of the guest is. Reduction in symmetry was also shown by solid-state photodimerization in the host-additive system of cinnamamide-cinnamic acid¹⁷ and will be discussed in this paper. Optical birefringence properties of crystals have also been taken advantage of

symmetry lowering in host-additive systems, as demonstrated by McBride and coworkers¹⁸⁻²⁰ who studied the molecular recognition at the growing surfaces of the tetragonal crystals of cis (11-bromoundecanoyl)peroxide ($\text{Br}(\text{CH}_2)_{10}\text{COOC}(\text{CH}_2)_{10}\text{Br}$) when grown in the presence of a guest where one of the two Br atoms is replaced by an H group (denoted as Br.....H). The mixed crystals contain as much as 15% Br.....H. The pure plate-like crystals are not birefringent for light traveling perpendicular to the plate. However the mixed crystals proved to be birefringent, indicating unsymmetrical incorporation of the Br.....H additives during crystal growth. McBride and Kahr¹⁸ related this observation to recent comprehensive studies by Akizuki and his collaborators, who explained optical anomalies of several minerals in terms of proposed differences among nominally symmetry-related unit cell sites at growth surfaces²¹⁻²³.

In all the host-additive systems, studied in our laboratory, the concentration of occluded additive was generally too low (maximally 1%) to permit detection of reduction in symmetry by X-ray or neutron diffraction measurements⁴. The question had arisen from our work on tailor-made additives whether a reduction in symmetry would occur in host-additive systems where the difference in molecular structure is sufficiently minor as to permit occlusion of additive, up to say 20%, and so be amenable to study by X-ray or neutron diffraction.

Symmetry lowering by O...O lone pair repulsion.

For this purpose we made use of solid solutions of guest carboxylic acids (XCO_2H) in host primary amides (XCONH_2), where the OH moiety is substituted for an NH_2 group^{17,24-26}. We had found, by neutron diffraction at low temperature (18K), that the symmetry of a solid solution of 15% carbon-deuterated aspartic acid in carbon-protonated asparagine is reduced to monoclinic $P12_11$: the symmetry of pure asparagine monohydrate is orthorhombic noncentrosymmetric $P2_12_12_1$. This reduction in symmetry^{4,25} was explained in terms of the preference of aspartic acid to avoid those surface sites on the {010} plate-like faces that would impose the lone-pair electrons of the guest hydroxyl oxygen atom, to form a repulsive O(hydroxyl)...O(carbonyl) contact^{3,27-29} with a host molecule. Normally, the O(carbonyl) participates in an (amide) N-H...O hydrogen bond. Incorporation of the acid in such an orientation would substitute a 2 kcal/mole (O...O) repulsion for a 6 kcal/mole N-H...O attraction³.

The detection of symmetry lowering in asparagine-aspartic acid by neutron diffraction would have been strongly masked had the effect of crystal sectoring not been taken into account. The specimen crystal was grown with only one of its two {010} plate like faces, through which the aspartic acid is selectively occluded, exposed to solution. A lack of awareness that symmetry lowering in solid solutions, when present, would occur in different sectors of the crystal, where the structures of these different sectors are related to each other by the point symmetry of the pure crystal, may be the essential factor why symmetry reduction was not observed long ago. However, as pointed out by Kahr and McBride¹⁸, anomalies in optical mineralogy had been noted over the years in which high symmetry minerals show division into sectors with lowered symmetry, but this phenomenon was usually attributed to strain fields or gross chemical segregation. Only as recently as 1988 Allen and Buseck, making use of optical and X-ray measurements on optically anisotropic grossular garnets, established that during growth selective incorporation of Fe³⁺ for Al³⁺ had lowered the symmetry of individual sectors³⁰.

For the amide-acid systems we next took advantage of the fact that centrosymmetric crystals possess chiral surfaces and that the selective occlusion of guest through these surfaces will cause a loss of the center of symmetry. Thus in a manner analogous to asparagine-aspartic acid, the additive E-cinnamic acid was found to induce a loss of the center of symmetry in the mixed crystal of E-cinnamamide¹⁷, which, in pure form, appears in a centrosymmetric monoclinic arrangement. The concentration of occluded guest was 1%; thus the reduction in crystal symmetry could not be reliably detected by X-ray or neutron diffraction. Hence the loss of the inversion symmetry was detected by asymmetric photodimerization between host and guest. Advantage was taken of the fact that cinnamamide forms close packed centrosymmetric pairs with a 4Å intermolecular separation between their C=C groups. In pure form cinnamamide yields centrosymmetric dimers **5** upon UV irradiation^{31,32}. Thus replacement of one of the molecules in the pair by cinnamic acid yields a chiral dimer, leading to an optically active photoproduct in a sector of the host-additive crystal.

Symmetry lowering by repulsion between lone pairs and π electrons.

The question then arose whether we could induce a reduction in crystal symmetry, where the repulsion between host and guest would be lower than between cinnamic acid and cinnamamide. The idea proposed, was to replace

the herring-bone contacts between the aromatic C-H groups and π electron clouds of neighboring phenyl rings of the cinnamamide **2** molecules by unfavorable contacts between lone-pair electrons and the π electron system. The electrostatic attraction of the C-H... π (cloud) interaction is supported by the already accepted idea that C-H bonds are sufficiently acidic to form attractive C-H...O hydrogen bonds^{33,34} coupled with the recent results of the microwave spectra of jet-cooled 1:1 clusters of benzene with water that demonstrate that both hydrogens of the water molecule point towards the π cloud with a distance of 3.3Å between the oxygen atom and the benzene ring³⁵. We chose the sulfur atom in the thienyl ring of thienylacrylamide **3**, to provide the lone pair electrons, for the following reasons. Solid solutions between molecules bearing phenyl and thienyl groups are well known³⁶. Evidence that the interactions between the lone pair lobes of the thienyl sulfur atoms and the aromatic π electron systems are repulsive is partially borne out by the fact that analogous compounds with and without sulfur atoms such as naphthalene³⁷ and thiophene³⁸, benzoic acid³⁹ and 2-thiophenic acid⁴⁰ are not isostructural; the sulfur lone pair- π electron interactions are not encountered in the sulfur containing analogues.

A reduction in crystal symmetry in cinnamamide 2-thienylacrylamide **3**, by selective occlusion of guest into a subset of symmetry related sites in appreciable concentration, say as low as 5%, would be clearly detectable by X-ray diffraction, because of the presence of the sulfur as a relatively strong X-ray scatterer. Neutron diffraction would also be a suitable probe, because the atoms of the host phenyl and guest thienyl rings do not coincide and one can also take advantage of the difference in the neutron scattering length of hydrogen and deuterium. Moreover it has been previously demonstrated that irradiation with light ($\lambda > 350$ nm) of a solid solution of cinnamamide : thienylacrylamide grown from the melt leads to the formation of the heterophotodimers⁴¹. In the mixed crystal there was no energy transfer from guest to host, so that the photoproduct distribution directly reflected the molecular occupancy of thienylacrylamide inside the cinnamamide crystal. Thus a loss of the crystal inversion symmetry, should yield an optically active photoproduct, in a manner akin to cinnamamide-cinnamic acid.

Cinnamamide crystallizes in the centrosymmetric space group $P2_1/c$ ($a=9.56$, $b=5.14$, $c=16.01$ Å, $\beta=94.1^\circ$) yielding prismatic crystals elongated in the b direction. When cinnamamide is crystallized in presence of additive 2-thienylacrylamide the morphology of the crystal changes (Fig.1).The four {011}

faces become more pronounced, implying that the thienyl molecules are occluded primarily through these faces. According to the space group and the structure of the crystal ($P2_1/c$) the four $\{011\}$ faces are not only chiral, but the two dimensional plane symmetry of each face is $p1$ and so exposes four independent surface sites, corresponding to the four symmetry related sites in the bulk, as shown in Figure 2. By virtue of the crystal point symmetry $2/m$ the two faces (011) and $(0\bar{1}\bar{1})$ are homochiral and congruent and enantiomeric to the $(0\bar{1}1)$ and $(0\bar{1}\bar{1})$ faces; related to the former by mirror symmetry. This structural property has already been described in the section under *Principles of reduction in symmetry*. Cinnamamide molecules at these $\{011\}$ faces display a herring-bone arrangement, which involves interactions between specific aromatic C-H groups and the π -electrons of neighboring phenyl rings. We envisaged that the desired site-selective adsorption and occlusion of guest thienylacrylamide molecules through these faces could be achieved through replacement of the "herring-bone" contact by unfavorable contacts between sulfur lone-pair electrons and the π electron system (Figure 3).

Consequently, as shown in Figure 4, 2-thienylacrylamide should be adsorbed most easily at site 1 on face $(0\bar{1}\bar{1})$, because the sulfur ring atom emerges from the crystal surface. The guest cannot occupy as easily site 2 at which the sulfur atom would point into the crystal bulk. At sites 3 and 4, the thienyl ring of a guest would lie almost parallel to the face and so there should be little difference in their relative ease of adsorption, but certainly a greater adsorption than at site 2 but less than at site 1. Any inequality in the average guest occupancy will result in reduction of symmetry; preferential occlusion at site 1 must yield space group $P1$. (An analogous symmetry lowering has also been shown schematically in the section under *Principles of reduction in symmetry*) Adsorption of thienylacrylamide takes place also through faces of type $\{001\}$, as revealed by changes in morphology. A selective occlusion through faces of this type should lead to symmetry Pc , given that the guest should be adsorbed more easily at sites 1,4 than at 2,3. As for guest occlusion through the two $\{100\}$ faces, examination of the packing arrangement suggested that absorption through all the four sites 1 - 4, should tend to be equally probable. Experimental considerations imposed upon us to make use of specimen crystals containing both (100) and $(\bar{1}00)$ faces, so that any reduction in crystal symmetry arising from minor differences in guest occlusion through these two faces would in any event be masked out. The mixed crystal may thus be divided in six sectors of reduced

symmetry (Figure 5), with the structure of the sectors related to each other by the $2/m$ point symmetry of the host crystal: the two joined sectors of symmetry $P1$ of type A at one half of the crystal along the symmetry axis b , will be congruent to each other and enantiomorphous to the two joined sectors of type \bar{A} at the opposite half. The two Pc sectors (type B), should have opposite polarity along the c axis.

On the basis of the photochemical and structural arguments presented, we anticipated that irradiation of a specimen crystal should yield the optically active dimers $4a$ and $4b$ of opposite chirality in excess in the sectors A and \bar{A} respectively. For example in the sector $\bar{A}(0\bar{1}1)$, delineated by the $(0\bar{1}1)$ face, thienylacrylamide guest molecules should populate site 1 more than site 2, and site 3 somewhat more than site 4. We note that the two sites within each pair 1 and 3, and 2 and 4 are related by twofold screw symmetry and that the two pairs are related by inversion symmetry. Thus thienylacrylamide at sites 1 and 3 will photoreact with cinnamamide at sites 2 and 4 to yield the chiral mixed dimer $4a$.

Results and Discussion

Diffraction analysis of cinnamamide-thienylacrylamide

Here we describe the results of the X-ray and neutron diffraction measurements and the crystal structure refinement of the mixed crystals of cinnamamide:2-thienylacrylamide. Complementary information of a more specialized nature, such as the neutron diffraction data collection, is presented in the experimental section.

Mixed crystals containing (host) cinnamamide and (guest) thienylacrylamide were grown from an ethyl acetate solution containing 30% guest. A concentration ranging from 7.5 to 8% guest was found occluded in the mixed crystals, according to HPLC (high performance liquid chromatography) measurements. For the X-ray diffraction study of the mixed crystals, a specimen was chosen from which a chip of regular dimensions 0.2 to 0.3 mm was cut from each of the two enantiomorphous (011) and (0 $\bar{1}$ 1) faces, as well as from the (001) face. The X-ray diffraction measurements were performed on these three crystal sectors, labeled *A* (011), \bar{A} (0 $\bar{1}$ 1) and *B* (001) cooled to a temperature of 100°K. To reduce systematic errors, in particular the effect of multiple X-ray diffraction, the Bragg reflections of each of the crystal sectors was measured in three different crystal orientations and the intensity data sets were subsequently averaged. To help facilitate the structure-factor least-squares refinement procedure of the mixed crystals X-ray diffraction measurements were also performed on crystals of pure cinnamamide and pure 2-thienylacrylamide cooled to a temperature of 100°K. The results of these X-ray experiments are summarized in Table 1. The crystals structures of pure cinnamamide and 2-thienylacrylamide were refined in a straightforward way, yielding fit indices [$R(F)=0.034$, $R_w(F)=0.046$] and [$R(F)=0.054$, $R_w(F)=0.066$] respectively.

The neutron diffraction measurements were performed on a pure cinnamamide crystal and on a large sector cut from a mixed cinnamamide (C-D deuterated) : thienylacrylamide (C-H protonated) crystal. The pure crystal was cooled to a temperature of 100°K. The cut sector of the mixed crystal, exposing an uncut (01 $\bar{1}$) face and so labeled *A* (01 $\bar{1}$), was cooled to a temperature of 200°K. Results are summarized in Table 2. Structure factor refinement of the pure crystal yielded $R(F^2)=0.038$.

Evidence in favor of a reduction from monoclinic to triclinic symmetry ($P1$) for each of the three sectors \bar{A} ($0\bar{1}1$), A (011) and A ($0\bar{1}\bar{1}$) was first apparent from the measurements of the unit cell angles α and γ in the pure and mixed crystals (Table 3), which in a monoclinic system would be 90° . According to Table 3 the deviations of the angle γ from 90° in the mixed crystal specimens are significant. The X-ray measurements yielded γ angles of $89.871(4)^\circ$ and $90.113(4)^\circ$ for the $A(011)$ and $\bar{A}(0\bar{1}\bar{1})$ sectors respectively. These two angles are complementary to each other in the sense that $\gamma(A) = 180 - \gamma(\bar{A})$ because the X-ray data of the two sectors from one crystal were measured with respect to the same axial system. A similar trend holds for the α angle, although here the deviation from 90° was minor; $\alpha(A)=90.018(6)^\circ$ and $\alpha(\bar{A})=89.969(20)^\circ$. The neutron diffraction measurements of an $A(0\bar{1}\bar{1})$ sector yielded $\gamma=90.114(2)^\circ$ and $\alpha=89.980(4)^\circ$. All these results are suggestive of a triclinic unit cell and an enantiomorphous relationship between the unit cells of A and \bar{A} and are striking in comparison to the measured angles of pure cinnamamide [$\alpha=89.999(2)^\circ$, $\gamma=90.008(2)^\circ$] and for those measured for the crystal sector $B(001)$ of anticipated monoclinic Pc crystal symmetry [$\alpha=89.998(2)^\circ$, $\gamma=90.005(2)^\circ$].

More concrete evidence in favor of space group $P1$ as against $P2_1/c$ for the A and \bar{A} crystal sectors is provided by the internal agreement factors R , between the observed symmetry-related X-ray reflections $F^2(hkl)$ assuming Laue point symmetry $\bar{1}$ as against $2/m$, which would correspond in the specimen crystals to triclinic and monoclinic symmetry respectively. The $R(F^2)$ values⁴² for the two point groups are [0.039, 0.044]⁴³ for crystal sector $\bar{A}(0\bar{1}\bar{1})$ and [0.041, 0.043]⁴⁴ for sector $A(011)$. The neutron diffraction measurements from crystal sector $A(0\bar{1}\bar{1})$ yielded [0.0265, 0.0398] for Laue symmetry $\bar{1}$ and $2/m$ respectively⁴⁵. These results are indicative of a loss of both the glide and twofold screw symmetry elements but not of the center of inversion, because the triclinic crystal may in principle exhibit $P\bar{1}$ symmetry.

A direct indication of the loss of the glide and twofold screw symmetries for crystal sectors $A(011)$ and $\bar{A}(0\bar{1}\bar{1})$ was provided by the presence of several of the symmetry "forbidden" X-ray reflections ($h0l$), $l=2n+1$ and ($0k0$), $k=2n+1$. A value of 5.3 was obtained for the ratio $I/\sigma(I)$ for the set of 150 symmetry forbidden reflections, where I is the net intensity and $\sigma(I)$ its estimated error. ψ scans⁴⁶ for several "symmetry"-forbidden X-ray reflections confirmed the presence of residual intensities despite the sometimes observed effect of multiple diffraction as shown in Fig 6. ψ scans of symmetry-forbidden neutron reflections on crystal

sector \bar{A} ($0\bar{1}1$) also confirmed the presence of residual, although weak, intensities (fig. 6). But we note that the relatively large size of the specimen crystal and the constant neutron scattering length for atoms as a function of $\sin \theta/\lambda$, increases the probability of multiple diffraction in the neutron experiments. The following procedure was adopted to establish, by crystal structure refinement, the symmetry of the crystal sectors A and \bar{A} . Essentially the same method was applied to the X-ray and the neutron diffraction data sets. The crystal structures of the A and \bar{A} sectors were refined by a structure-factor least-squares procedure, first assuming $P2_1/c$ symmetry. A "composite" molecule was constructed from a cinnamamide molecule and a 2-thienyl moiety. The molecular geometries of these two components were taken from their pure low-temperature crystal structures. The two molecules were treated as rigid bodies with constraints imposed on their overlap, atomic displacement parameters and occupancies⁴⁷. The crystal structure refinements assuming $P2_1/c$ symmetry yielded fit indices $R(F)$ of 0.042 and 0.045 for the two sectors A (011) and \bar{A} ($0\bar{1}1$) studied by X-rays and 0.0482 for the A ($01\bar{1}$) sector studied by neutrons. The respective host-guest occupancies of sectors $A(011)$ and $\bar{A}(0\bar{1}1)$ of [0.922(2), 0.0780(3)] and [0.923(2), 0.077(2)] are in good agreement with the concentration of thienylacrylamide as determined by HPLC measurements on these specimen crystals. These three crystal structures were then refined with $P1$ symmetry. The number of variables were kept to a minimum by retaining the refined geometry and the values of the atomic displacements parameter U_{ij} of the $P2_1/c$ structure and refining only the overall scale factor and the relative host-guest occupancy of each of the four "symmetry"-related composite molecular sites in the unit cell⁴⁸. The resulting X-ray and neutron crystal structure refinements yielded $R(F)$ fit indices of 0.038, 0.040 and 0.0475 for the \bar{A} ($0\bar{1}1$), A (011) and A ($01\bar{1}$) sectors respectively. These values are lower than the corresponding fit indices for the $P2_1/c$ model structure (vide supra 0.042, 0.045, 0.0482), but do the refined molecular occupancies make chemical sense in terms of the proposed model of adsorption and occlusion through the $\{011\}$ faces? The guest occupancies of each of the four sites 1, 2, 3, 4, for the three crystal sectors are listed in Table 4. We compare the occupancies of the four molecules with their orientations relative to the corresponding $\{011\}$ face through which the guest molecules were occluded into the crystal. To facilitate this comparison we refer all occupancies to that of crystal sector \bar{A} ($0\bar{1}1$), by applying the appropriate point symmetry element to molecules 1, 2, 3, 4. For example the four (1, 2, 3, 4) sites

at face (011) would transform to sites 4, 3, 2, 1 respectively by application of m symmetry. The most significant difference in occupancy corresponds to the two sites related by inversion symmetry at which the thienyl ring is almost perpendicular to the plane of the {011} face through which the guest was occluded. For sector \bar{A} ($0\bar{1}1$) this corresponds to sites 1 and 2. The average guest occupancies for such sites in the three crystal sectors are 0.146 and 0.016. The two sites with the smallest difference in occupancy are those related by a center of inversion, at which the thienyl ring needs to be parallel to the plane of the {011} face through which the guest was occluded. For sector \bar{A} ($0\bar{1}1$) this corresponds to sites 3 and 4. The average guest occupancies for these types of sites in the three crystals sectors are 0.066 and 0.063. These occupancies at the four sites are in keeping with the proposed mechanism of preferred adsorption and occlusion of guest into the crystal through the four {011} faces, but for one remaining and central ambiguity. The X-ray diffraction data were not sufficiently accurate to allow us to assign the absolute configuration of the crystal sectors. The same fit index $R(F)$ was obtained for the two crystal sectors \bar{A} ($0\bar{1}1$) and A (011) upon generating the inverted crystal structure by reversing the signs of all xyz atomic coordinates. Moreover a comparison of the intensities of Bijvoet pairs, $I(hkl)$ and $I(\bar{h}\bar{k}\bar{l})$ of selected X-ray reflections did not allow us to ascertain the absolute configuration of the specimen crystals. Thus although the X-ray and neutron diffraction studies have demonstrated the reduction in crystal symmetry to $P1$ for the A and \bar{A} sectors, they do not yield the orientation of preferred adsorption of guest through the {011} faces. An analogous question was readily answered in the neutron diffraction study of (S) Asparagine-(S) Aspartic acid²⁵, because the absolute configuration of the molecule and thus the crystal was known. The ambiguity in the case of cinnamamide-thienylacrylamide was resolved by assignment of the absolute configuration of the chiral hetero photodimers in excess in the A -type crystal sectors, described in the next section. An examination of reduction of crystal symmetry for the B (001) sector was not conclusive as for the A and \bar{A} sectors. For example the ψ scans of the "symmetry"-forbidden $0k0$ $k=2n+1$ reflections did not reveal the presence of net intensities. The crystal structure of the B (001) sector was refined in a manner analogous to that of the A and \bar{A} sectors. Fit indices $R(F)$ of 0.044 and 0.0435 were obtained for the space groups $P2_1/c$ and Pc respectively. The occupancies of sites 1, 4 and 2, 3 for space group Pc were 0.100(1) and 0.039(1) respectively. Although the difference in occupancies of the two sets of sites appears to be

statistically significant, there was not corroborating evidence for reduction in crystal symmetry, as was found for the *A* and \bar{A} sectors.

Assignment of Absolute Configuration of the Mixed Crystal Segments by Solid State Photodimerization

In accordance with the X-ray and neutron diffraction results irradiation with monochromatic light of sectors *A* and \bar{A} cut from single crystals yielded optically active photodimers *4a* and *4b*. Circular dichroism and gas chromatography on a chiral column, showed that the photoproducts obtained in excess from the *A* and \bar{A} type sectors are enantiomers with an e.e. in the range of 40-69% (Figure 8 and Figure 9)

As expected, photoirradiation of sector *B* of the crystal yields a racemic mixture of both enantiomers.

In order to determine the absolute configuration of the dimers *4a* and *4b*, the S-(+)-sec-butyl diesters of the products obtained from sector *A* and \bar{A} were prepared. According to HPLC analyses the mixtures consisted of about 90% heterodimer diester *4*, about 7% of truxillic diester *5* and 3% of dithiophenediester *6*. Assuming, that the spectrum of the heterodimer diester is a combination of the spectra of the truxillic acid di-S-(+)-sec-butyl diester and the corresponding dithiophene dimer diester (Figure 10), then the peaks of relevance are the doublets at 0.92 and 1.01 ppm respectively. These doublets don't overlap and so their intensities can yield which enantiomer is present in excess. These peaks belong to the methyl group *A* of the sec-butyl at C(1), of absolute configuration *S* and to methyl group *A* of the sec-butyl at C(3), which has absolute configuration *R*. The doublets undergo deshielding from the neighboring aromatic ring in the *cis* position. The homodimer molecules lost the center of inversion, because of esterification with S-(+)-sec-butanol and thus have absolute configuration 1*S*,2*R*,3*R*,4*S*. The ratio of the doublets at 0.92 and 1.01 ppm in the spectrum of the diesters of material isolated from sector *A* was 6:4, after correction for the presence of homodimers (Figure 11a). This result indicates that the enantiomer with absolute configuration *R* at C(3), in which the ester group is *cis* to the phenyl ring and absolute configuration *R* at C(1), in which the ester group is *cis* to the thienyl ring, is found in excess. Thus enantiomer *4a* of absolute configuration 1*R*,2*S*,3*R*,4*R* is formed in excess in segment *A* at the +*b* end of the crystal. Likewise, the ratio of the

doublets in the spectrum of the diesters of material isolated from sector \bar{A} was 4:6 (Figure 11b). Thus dimer *4b* with absolute configuration 1S,2R,3S,4S is formed in excess in segment \bar{A}

Conclusion

The reduction in crystal symmetry of solid solutions depends upon molecular recognition at the surfaces of the growing crystal. The principles are thus applicable to all molecular crystals, be they organic, inorganic or crystals containing biological macromolecules. The symmetry lowering provides a powerful tool for probing subtle molecular interactions. In the present study we have demonstrated symmetry lowering in different sectors of the specimen crystals arising from intermolecular repulsion between lone pair electrons and π electron clouds. The cumulative evidence is now overwhelming that mixed single crystals composed of host and guest molecules of similar structure and shape can comprise sectors with different host-guest distributions and symmetries lower than that of the host crystal.

Experimental.

CD spectra were measured with a Jasco 500 spectrophotometer. UV spectra were measured on a Hewlett Packard 8450A diode array spectrophotometer. NMR spectra were recorded on a Bruker 270 MHz spectrometer. GC spectra were made on a Hewlett Packard 5890 gas chromatograph equipped with a 25m. fused silica Chirasil-L-Valine capillary column (purchased from Chrompack) at 180°C, with 0.9 bar carrier gas (He) and FID detection. HPLC analyses were done on a Waters HPLC equipped with a 240x4.6mm Rp 18 chromosorb 5 μ m column; the eluent was 40% acetonitrile in buffer acetate 0.05M pH 3.9 at flowrate 1ml/min for the monomers and 25% acetonitrile for the reaction mixture. TLC was done on silica in toluene:dioxane:acetic acid 200:50:8. The detection was done by UV and sprayed with 2.6 dichlorophenolindophenol (80mg/100ml ethanol) or with isatin (0.4 gr/100ml H₂SO₄ 97% in order to detect the thiophene containing compounds). The R_f for phenyl ring and thienyl ring containing compounds under these conditions are identical. However on

Rp 8 TLC plates, 40% acetonitrile or methanol in buffer acetate pH 4.0 0.05M when run twice, separation is possible. For the diester mixtures TLC was done on silica with 5% ethyl acetate in hexane as eluent. HPLC analyses of the S-(+)-sec-butyl diesters of 4 were performed on a 10 cm. Rp 18 column with eluent 30% water in acetonitrile at flowrate 0.5 ml/min (HP 1050 quaternary pump, Jasco 875 UV/Vis detector, HP integrator).

Preparation of materials. Cinnamamide was obtained via the acylchloride and reaction with ammonia, as described for the preparation of amides in Vogel's textbook of Practical Organic Chemistry.

2-thienylacrylamide and 3-thienylacrylamide were prepared according to the same methods from the corresponding acids, recrystallized from ethyl acetate and sublimed.

2-thienylacrylic acid was prepared by condensation of thiophene-2-carboxaldehyde (1/3 mole) with malonic acid (3/4 mole) 150ml pyridine with 2.5ml piperidine.

3-thienylacrylic acid was prepared by the same method from thiophene-3-carboxaldehyde.

Derivatization of materials for GC. The retention times for the thienyl and phenyl ring containing compounds are identical on the Chirasil-L-Valine column. Thus the mixture to be analyzed was refluxed in ethanol with Raney Nickel (which was prepared according to Fieser and Fieser, vol 1), for 2 days. Afterwards the reduced reaction mixture was filtered and the solvent evaporated and reacted with 25% trifluoroacetic anhydride in methylene chloride for 1hr at 0°C.

Preparation of the optically active sec-butyl esters of compound 4. The thienyl phenyl heterodimer 4 was refluxed for 48 hrs with methanol /HCl, after which the solvent was evaporated. The crude reaction product was dissolved in methylene chloride, extracted with water, sodium bicarbonate solution and water. Afterwards the methylene chloride fraction was dried over MgSO₄ and evaporated. The mixture which also contained monomer Methyl ester was cleaned by flash chromatography on a 1 cm Ø silica column with 5% ethyl acetate in hexane as eluent. The clean methyl ester was transesterified with S-(+)-butanol/HCl during 24 hrs reflux and followed by identical workup as described for the methyl ester. Although the material

was nearly completely clean according to TLC, it was cleaned on a small silica column with 2.5% ethyl acetate in hexane.

NMR: All spectra were recorded at a 270 Mhz spectrometer unless otherwise mentioned.

thiophene phenyl heterodimer 4; ^1H NMR ($(\text{CD}_3)_2\text{SO}$) δ 3.85-3.97 (m, 1H), 3.98-4.1 (m, 1H), 4.45-4.69 (m, 1H), 4.64-4.69 (m, 1H), 7.00-7.06 (m, 2H, H3 and H4 of thiophene ring), 7.25-7.45 (m, aromatics 6H).

truxillic acid diamide 5 ^1H NMR ($(\text{CD}_3)_2\text{SO}$) δ 4.0-4.1 (m, 2H), 4.4-4.55 (m, 2H), 7.2-7.5 (m, aromatics 10H).

dithiophene diamide 6 ^1H NMR ($(\text{CD}_3)_2\text{SO}$) δ 3.88-4.0 (m, 2H), 4.69-4.80 (m, 2H), 6.9-7.1 (m, 4H), 7.25-7.4 (m, 2H).

truxillic acid dimethyl ester; ^1H NMR (80 MHz, CD_2Cl_2) δ 3.21 (s, 6H), 3.8-4.0 (m, 2H), 4.2-4.4 (m, 2H), 7.3 (br s, 10H).

dithiophene dimethyl ester; ^1H NMR (80 MHz, CD_2Cl_2) δ 3.27 (s, 6H), 3.5-3.9 (m, 2H), 4.3-4.6 (m, 2H), 6.9-6.9 (m, 4H), 7.08-7.12 (m, 2H).

Dithiophene di S(+)-2-butylester ; ^1H NMR (CD_2Cl_2) δ 0.58 (tr, 3H), 0.69 (d, 3H), 0.76 (tr, 3H), 1.01 (d, 3H), 1.13-1.25 (m, 2H), 1.32-1.47 (m, 2H), 3.75-3.85 (m, 2H), 4.5-4.65 (m, 4H), 6.89-6.97 (m, 4H), 7.16-7.20 (m, 2H).

Truxillic acid di-S(+)-2-butylester₁ ^1H NMR (CD_2Cl_2) δ (0.52, tr), 0.58 (d, 3H), 0.74 (tr, 3H), 0.92 (d, 3H), 1.06-1.15 (m, 2H), 1.22-1.42 (m, 2H), 3.82-3.97 (m, 2H), 4.32-4.58 (m, 4H), 7.2-7.3 (m, 2H), 7.3-7.4 (m aromatics 8H)

Di-(S)(+)-2-butylester of 6 ^1H NMR (CD_2Cl_2) δ 0.45-0.70 (m, consisting of tr, d and tr), 0.65-0.80 (m, consisting of tr, d and tr), 0.92 (d, 3/2H), 1.01 (d, 3/2H) 1.08-1.5 (2 m, 4H), 3.75-3.85 (m, H), 3.85-3.97 (m, H), 4.3-4.48 (m, 2H), 4.48-4.65 (m), 6.9-7.0 (m, 2H at position 3 and 4 of the thienyl ring), 7.15-7.4 (m, aromatics 6H).

Crystal growth.: Small crystals were grown in beakers by slow evaporation at room temperature, 200 mgr cinnamamide with 20,40 or 60 mgr thienyl acrylamide in 10ml ethyl acetate. Crystals of pure 2-thienylacrylamide were grown from a solution of 240 mgr/15ml ethyl acetate. Large crystals used for the reactions were grown in erlenmeyers from 3.5 gr of cinnamamide with 700 mgr 2-thienyl acrylamide in 100 ml ethyl acetate. As seed crystals, cinnamamide grown in presence of αCl -cinnamic acid, were used because they tend to develop large {110} faces. A seed crystal was placed in each

erlenmeyer. The vessels were kept in a thermostated water bath, whose temperature was lowered from 45°C by 1°C per day until the crystals were large enough or 30°C was reached.

Preparation for irradiation.: As described in Chapter 2, but the petridishes were covered with "filters", i.e. a film of molten cinnamamide between two glass slides or filters that cut off $\lambda > 350\text{nm}$. The petri dishes were irradiated with sunlight or sunlamps.

Isolation of the dimers.: The dimers were isolated by dissolution of the irradiated material in ethyl acetate followed by precipitation with hexane. The precipitate was enriched in dimer. For the preparation of the diesters for NMR, the enriched material was used without further cleaning. For GC chromatography and C.D analysis, purification was continued in order to remove all the monomer by T.L.C. or P.L.C. in toluene:dioxane:acetic acid = 200:50:8.

Neutron Diffraction Data Collection

The neutron diffraction measurements were carried out at the Brookhaven high-flux beam reactor using a computer controlled four circle goniometer. The neutron beam was monochromated by reflection from a Ge or Be crystal. The specimen crystals were mounted in an aluminum canister and placed inside a closed-cycle helium refrigerator. The crystals were then gradually cooled down to the appropriate temperature. Details of the neutron diffraction data measurements on cinnamamide and cinnamamide-thienylacrylamide are given in Table 2. Crystal absorption corrections were calculated using crystal dimensions⁴⁹. Crystal extinction corrections were applied in the structure-factor least-squares program. Initial refinement of pure cinnamamide was carried out using a differential synthesis program⁵⁰, followed by least-squares with the program UPALS⁵¹. Description of the refinement of the mixed cinnamamide-thienylacrylamide crystal is given in the main text.

SUPPLEMENTARY MATERIAL available, these include fractional atomic coordinates and temperature factors of pure cinnamamide, 2-thienylacrylamide and of the mixed crystal cinnamamide-thienylacrylamide at 100°K.

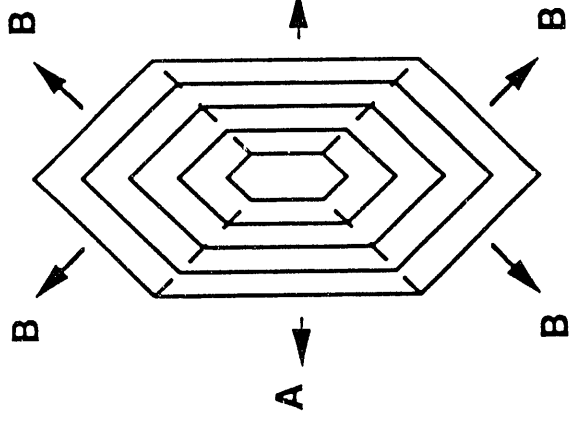
Acknowledgment This research was carried out, in part, at Brookhaven National Laboratory under Contract DE-AC02-76CH00016 with the U.S. Department of Energy and supported by its Office of Basic Sciences. We are grateful to the U.S./Israel Binational Foundation, Jerusalem for financial support

References

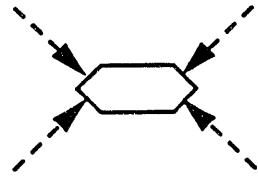
- (1) L. Addadi, Z. Berkovitch-Yellin, I. Weissbuch, M. Lahav, L. Leiserowitz and S. Weinstein *J. Am. Chem. Soc.* 1982, **104**, 2075-2077.
- (2) L. Addadi, Z. Berkovitch-Yellin, N. Domb, E. Gati, M. Lahav and L. Leiserowitz *Nature* 1982, **296**, 21-26.
- (3) L. Addadi, Z. Berkovitch-Yellin, I. Weissbuch, J. v. Mil, L. J. W. Shimon, M. Lahav and L. Leiserowitz *Angew. Chem., Int. Ed. Engl.* 1985, **24**, 466.
- (4) L. Addadi, Z. Berkovitch-Yellin, I. Weissbuch, M. Lahav and L. Leiserowitz In *Topics in Stereochemistry*, E. L. Eliel, S.H. Willen and N. L. Allinger, Ed.; John Wiley & Sons Inc.: New York, 1986; Vol. 16; pp 1-85.
- (5) Z. Berkovitch-Yellin, L. Addadi, M. Idelson, L. Leiserowitz and M. Lahav *Nature* 1982, **296**, 27-34.
- (6) I. Weissbuch, L. Addadi, Z. Berkovitch-Yellin, E. Gati, S. Weinstein, M. Lahav and L. Leiserowitz *J. Am. Chem. Soc.* 1983, **105**, 6613.
- (7) I. Weissbuch, L. Addadi, Z. Berkovitch-Yellin, E. Gati, M. Lahav and L. Leiserowitz *Nature* 1984, **310**, 161.
- (8) I. Weissbuch, L. J. W. Shimon, L. Addadi, Z. Berkovitch-Yellin, S. Weinstein, M. Lahav and L. Leiserowitz *Isr. J. Chem.* 1985, **25**, 353-362.
- (9) I. Weissbuch, Z. Berkovitch-Yellin, L. Leiserowitz and M. Lahav *Isr. J. Chem* 1985, **25**, 362-372.
- (10) M. Vaida, L. J. W. Shimon, Y. Weisinger-Léwin, F. Frolow, M. Lahav, L. Leiserowitz and R. K. McMullan *Science* 1988, **241**, 1475.
- (11) M. Vaida, I. Weissbuch, M. Lahav and L. Leiserowitz *Isr. J. Chem* 1992, **32**, 15-21.
- (12) M. Vaida, R. Popovitz-Biro, L. Leiserowitz and M. Lahav In *Photochemistry in Organized and Constrained Media*; V. Ramamurthy, Ed.; VCH Publishers Inc.: New York, 1991; pp Chapter 6, p. 247-302.
- (13) I. Weissbuch, L. Addadi, M. Lahav and L. Leiserowitz *J. Am. Chem. Soc.* 1988, **110**, 561-567.
- (14) The symbol $2/m$ specifies a twofold axis perpendicular to a mirror plane, the combination of which generates a center of inversion.
- (15) P. Curie *J. Phys. (Paris)* 1894, 393.
- (16) I. Weissbuch, M. Lahav, L. Leiserowitz, G. R. Meredith and H. Vanherzeele *Chemistry of Materials* 1989, **1**, 14.

- (17) M. Vaida, L. J. W. Shimon, J. v. Mil, K. Ernst-Cabrera, L. Addadi, L. Leiserowitz and M. Lahav *J. Am. Chem. Soc.* 1989, **111**, 1029.
- (18) B. Kahr and J. M. McBride *Angew. Chem. Int. Ed. Engl.* 1992, **31**, 1-26.
- (19) J. M. McBride and S. B. Bertman *Angew. Chem. Int. Ed. Engl.* 1989, **28**, 330.
- (20) J. M. McBride *Angew. Chem. Int. Ed. Engl.* 1989, **28**, 377.
- (21) M. Akizuki and I. Sunagawa *Mineral. Mag.* 1978, **42**, 453.
- (22) M. Akizuki and H. Konno *N. Jahrb. Min. Abh.* 1985, **151**, 99.
- (23) M. Akizuki *Am. Mineral.* 1987, **72**, 645-648.
- (24) J. L. Wang, Z. Berkowitz-Yellin and L. Leiserowitz *Acta Cryst.* 1985, **B41**, 341-348.
- (25) Y. Weisinger-Lewin, F. Frolow, R. K. McMullan, T. F. Koetzle, M. Lahav and L. Leiserowitz *J. Am. Chem. Soc.* 1989, **111**, 1035.
- (26) M. Vaida Ph.D. Thesis, Weizmann Institute of Science, Rehovot, Israel, 1990.
- (27) Z. Berkovitch-Yellin and L. Leiserowitz *J. Am. Chem. Soc.* 1982, **104**, 4052-4064.
- (28) C. Huang, L. Leiserowitz and G. M. J. Schmidt *J. Chem. Soc. Perkin 2* 1973, 503.
- (29) L. Leiserowitz *Acta Cryst.* 1976, **B32**, 775.
- (30) F. M. Allen and P. R. Buseck *Am. Mineral.* 1988, **73**, 568-584.
- (31) G. M. J. Schmidt *J. Chem. Soc.* 1964, **385**, 385.
- (32) M. D. Cohen, G. M. J. Schmidt and F. I. Sonntag *J. Chem. Soc.* 1964, **384**, 2000.
- (33) Z. Berkovitch-Yellin and L. Leiserowitz *Acta Cryst.* 1984, **B40**, 159-165.
- (34) R. Taylor and O. Kennard *J. Am. Chem. Soc.* 1982, **104**, 5063-5070.
- (35) S. Suzuki, P. G. Green, R. E. Bumgarner, S. Dasgupta, W. A. G. III and G. A. Blake *Science* 1992, **257**, 942-945.
- (36) J. D. Hung, M. Lahav, M. Luwish and G. M. J. Schmidt *Isr. J. Chem.* 1972, **10**, 585.
- (37) S. C. Abrahams, J. M. Robertson and J. G. White *Acta Cryst.* 1949, **2**, 238.
- (38) E. G. Cox, R. J. J. H. Gillot and G. A. Jeffrey *Acta Cryst.* 1949, **2**, 356.
- (39) R. Feld, M. S. Lehman, K. W. Muir and W. C. Speakman *Z. Kristallogr.* 1981, **157**, 215.
- (40) G. J. Visser, G. J. Heeres, J. Wolters and A. Vos *Acta Cryst.* 1968, **B24**, 467.

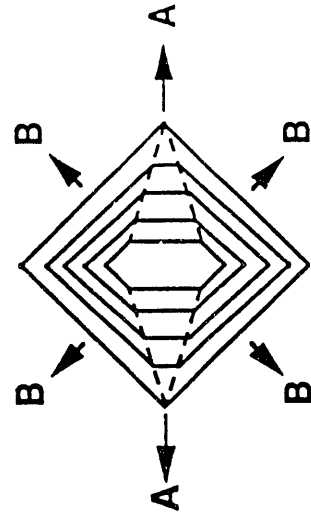
- (41) M. D. Cohen, R. Cohen, M. Lahav and P. L. Nie *J. Chem. Soc.* 1972, 1095.
- (42) $R_m(F^2)$ is defined in table 1.
- (43) The total number of reflections was 13306 for the crystal measured in three different orientations. The number of independent reflections, assuming point symmetry $\bar{1}$ (i.e. after averaging Friedel pairs), was 2231. The number of independent reflections, assuming $2/m$ point symmetry was just over half the value of 2231.
- (44) In a manner akin to the previous reference, the total number of reflections for the A(011) sector was 11111 yielding 2232 independent reflections assuming $\bar{1}$ point symmetry. The number of independent reflections of $2/m$ symmetry was just over half of that number.
- (45) Assuming $\bar{1}$ point symmetry only 241 Friedel pairs $I(okl)$ and $I(o\bar{k}\bar{l})$ were averaged. Assuming $2/m$ point symmetry yielded a total of 2171 averaged reflections, i.e. from $I(hkl)$ and $I(h\bar{k}\bar{l})$.
- (46) In a ψ scan about a reciprocal vector $d^*(hkl)$, the crystal is rotated about $d^*(hkl)$ in diffracting position. The diffraction intensity is then measured as a function of this rotation.
- (47) For the X-ray data 87 parameters were refined, whereas 134 parameters were refined for the neutron data. The latter included refinement of extinction parameters as well as a somewhat more relaxed model. Note that the number of reflections included the symmetry-related (hkl) and $(h\bar{k}\bar{l})$ reflections.
- (48) The total number of parameters refined were thus 5. Note that the complete set of reflections was used including the "symmetry forbidden" $(h0l)$ $l=2n+1$ and $(0k0)$ $k=2n+1$ reflections. Note that although the total number of neutron reflections was 4618, 1734 were suppressed from the least-squares, because they have $F/\sigma(F) < 6$.
- (49) J. D. Meulenaer and H. Tompa *Acta Cryst.* 1965, **19**, 1014.
- (50) R. K. McMullan "DIFSYN, a program for crystal structure refinement by the method of fourier synthesis," Brookhaven National Laboratory, Upton, N.Y., U.S.A., 1976 (unpublished).
- (51) J. O. Lundgren "UPALS. Least squares refinement program for crystal structures," Institute of Chemistry, University of Uppsala, Uppsala, Sweden, 1982.



Unaffected crystal growth
rate of growth $B > A$

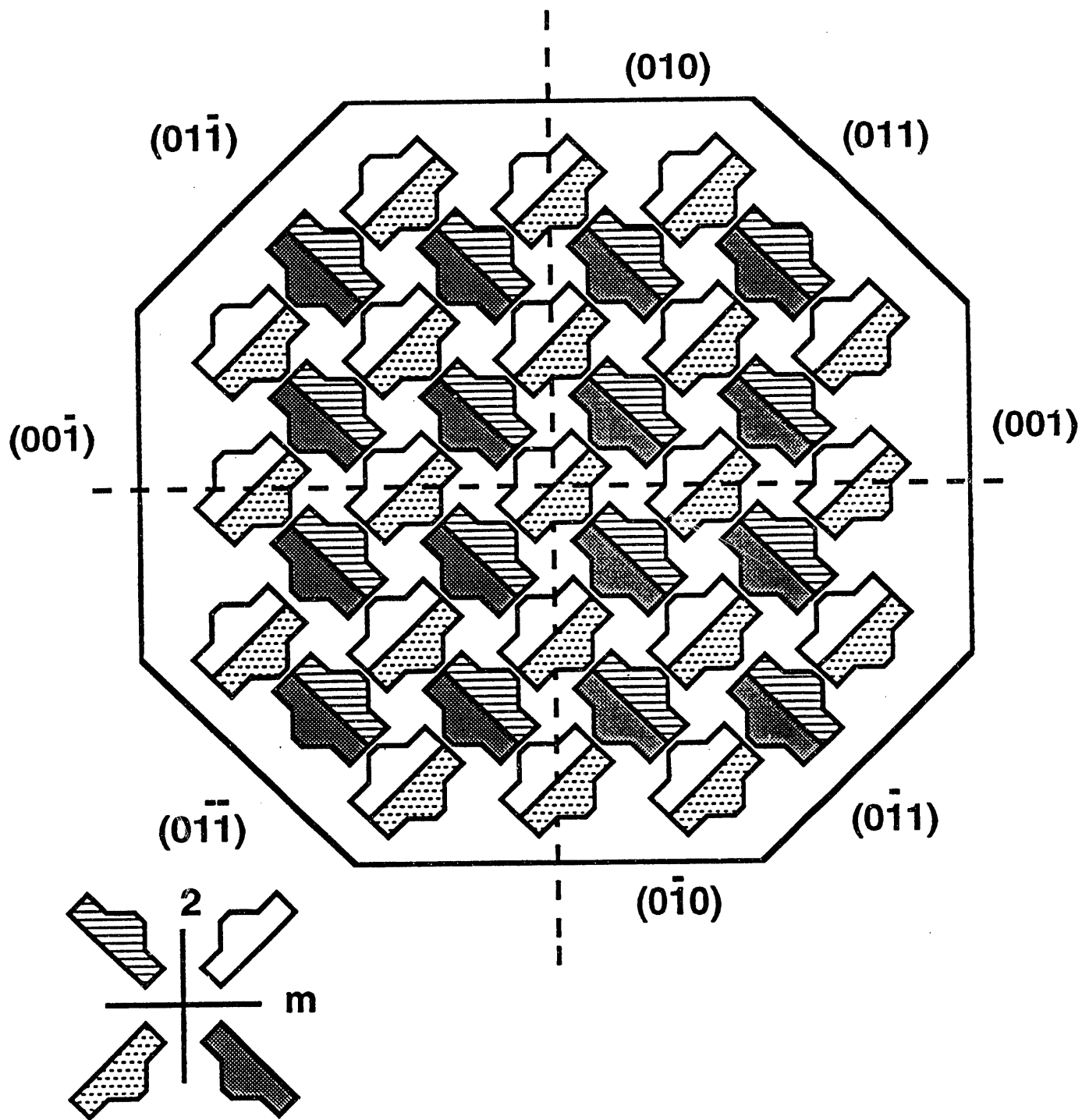


Stereoselective adsorption
of additive inhibits the
growth of the B faces

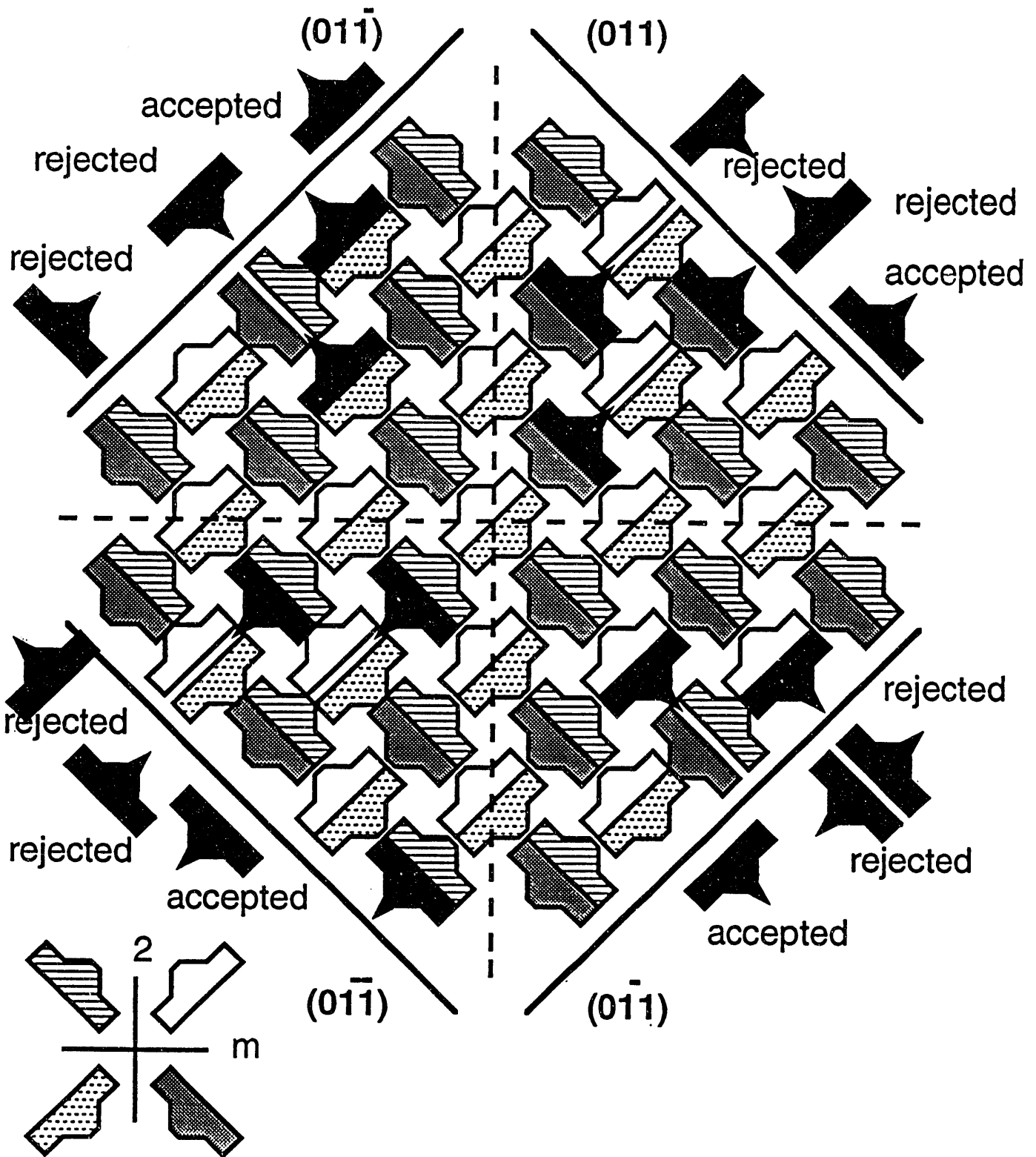


Affected crystal growth
rate of growth $A > B$

Scheme 1



Scheme 2



Scheme 3

- Figure 1: Morphology of cinnamamide; (left) pure; (right) grown in the presence of 2-thienylacrylamide.
- Figure 2: Packing arrangement of (E)-cinnamamide. View along the a axis. The $\{011\}$ faces are shown and the four symmetry related sites (1-4) are denoted.
- Figure 3: Herring-bone contacts between: (a) an adsorbed 2-thienyl acrylamide molecule and a cinnamamide molecule; (b) two cinnamamide molecules.
- Figure 4: Packing arrangement of cinnamamide at the $(0\bar{1}1)$ face, showing the four different surface sites. The filled atoms are those of 2-thienyl rings in the positions they would assume were they to replace cinnamamide molecules.
- Figure 5: Morphological representation of a cinnamamide crystal, with sectors of reduced symmetry.
- Figure 6: X-ray diffraction scans about the d^* (hkl) vector (ψ scan) of the $(60\bar{5})$, $(10\bar{1})$ and $(20\bar{7})$ reflections of sector $\bar{A}(0\bar{1}1)$ and of the (007) and (003) reflection of sector $A(011)$, showing integrated intensities (■) and background (○) for all measurable values of ψ . At some points along the ψ scans very high intensities were recorded, arising from multiple X-ray diffraction. These points are not indicated.
- Figure 7: Gas chromatogram of the O-iPr-N-TFA derivatives of compounds $4a$ and $4b$ of sectors A , \bar{A} and B . The thiophene ring was reduced to an n-butyl group (Chirasil-L-valine capillary column.)
- Figure 8: Circular dichroism spectra of photodimers $4a$ and $4b$ obtained from sectors A and \bar{A} respectively.
- Figure 9: NMR spectrum of the methyl regions of:

(a) The di S-(+)-sec-butyl ester of **6**. By esterification the compound lost its center of inversion and became chiral of absolute configuration 1S,2R,3R,4S.

(b) The corresponding diester of **5**. This compound also has absolute configuration 1S,2R,3R,4S. The doublets at 1.01 and 0.92 ppm respectively, belong to methyl group A of the sec-butyl ester at C1, which has absolute configuration S.

Figure 10: NMR spectrum of the methyl region of

(a) The S-(+)-sec-butyl diester mixture of the material isolated from an *A* sector, which consists of 90% heterodimer **4**. The ratio of doublet A₁:A₃ is 4:6, meaning that the diastereomer in excess is 1*R*,2*S*,3*R*,4*R*, **4a**.

(b) The corresponding diester of the material isolated from an \bar{A} sector, which also consists of 90% heterodimer **4**. In this case the ratio of doublet A₁:A₃ is 6:4, meaning that the diastereomer in excess is 1*S*,2*R*,3*S*,4*S*, **4b**.

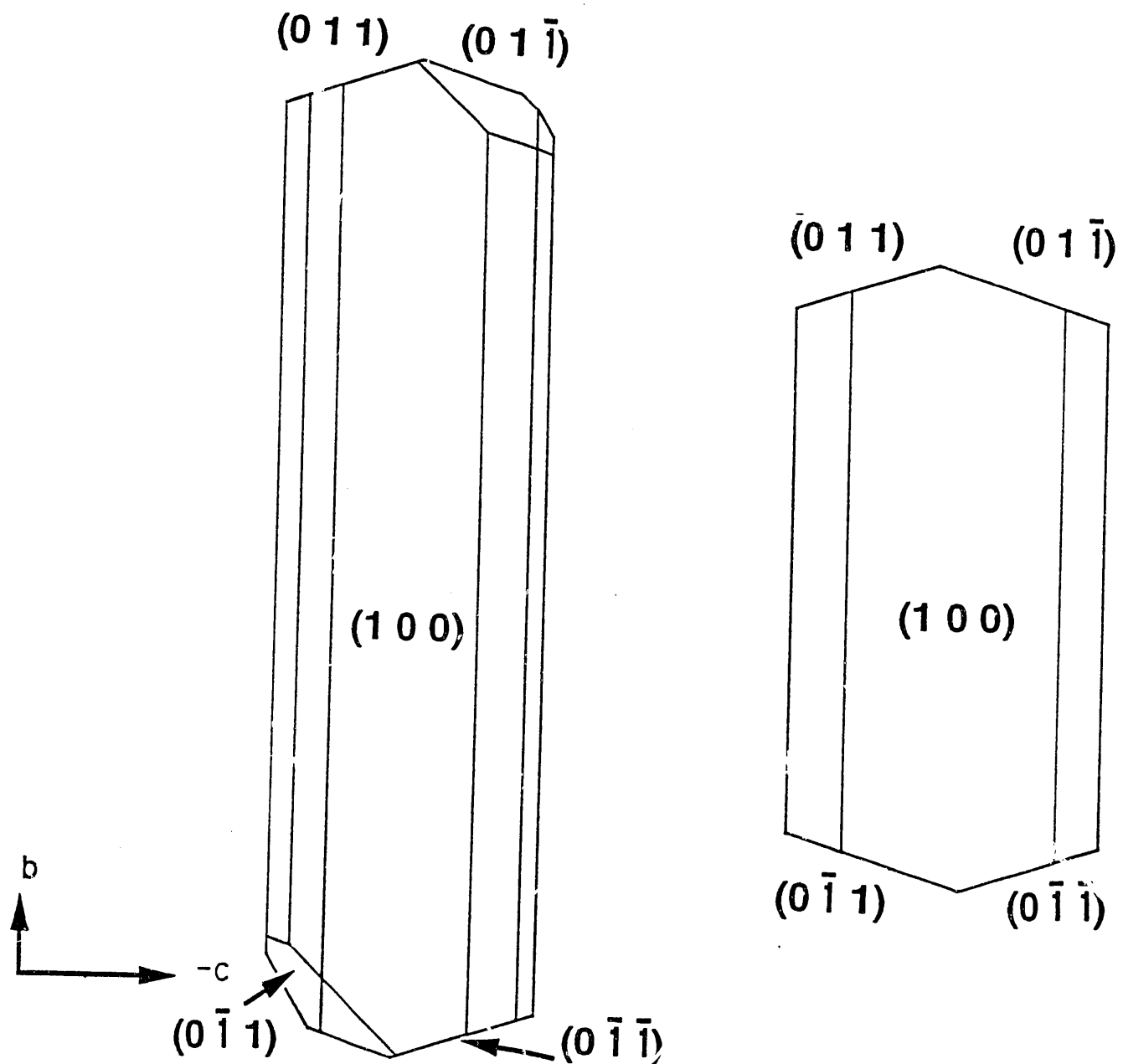


Figure 1: Morphology of cinnamamide; (left) pure; (right) grown in the presence of 2-thienylacrylamide.

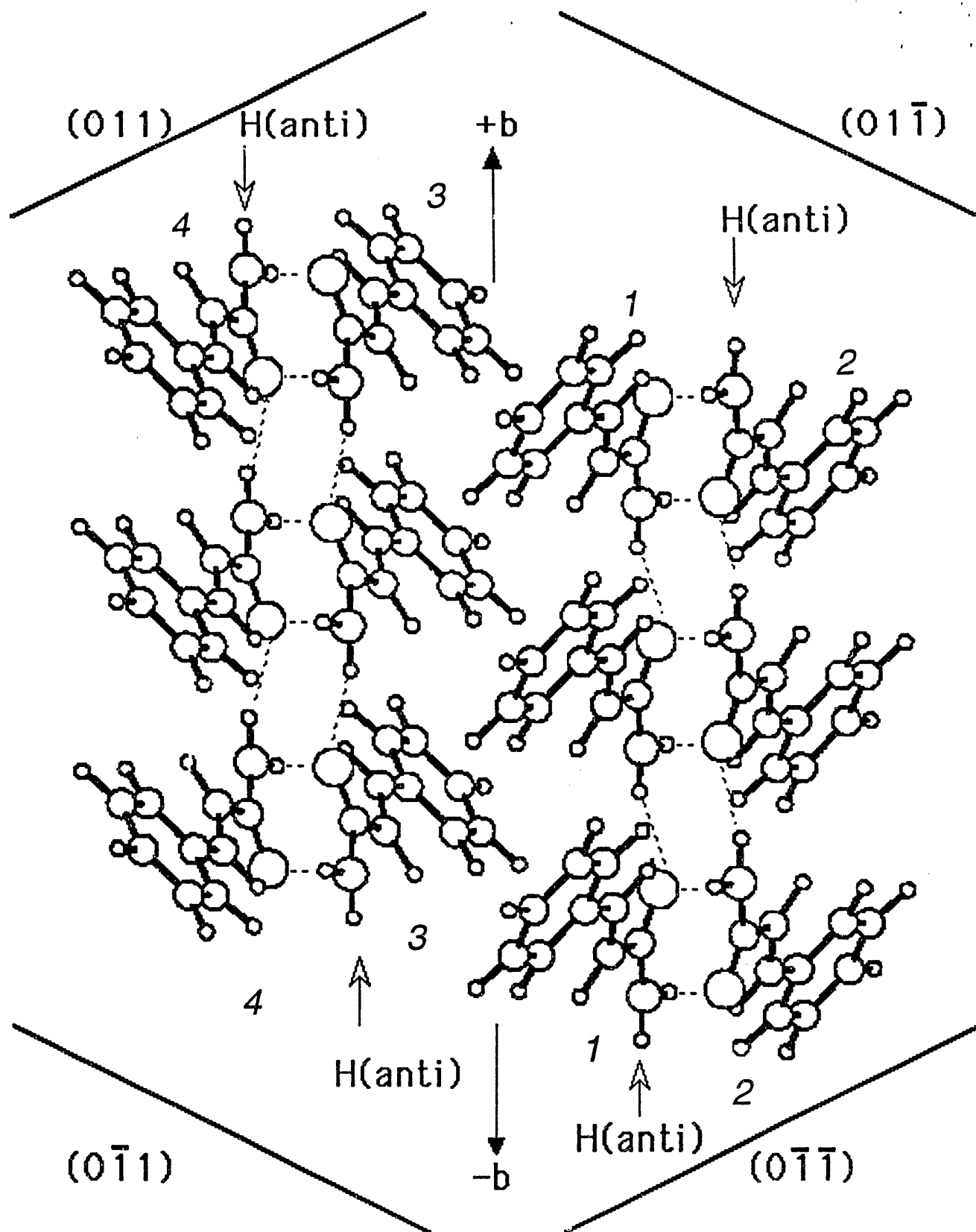


Figure 2: Packing arrangement of (E)-cinnamamide. View along the *a* axis. The {011} faces are shown and the four symmetry related sites (1-4) are denoted.

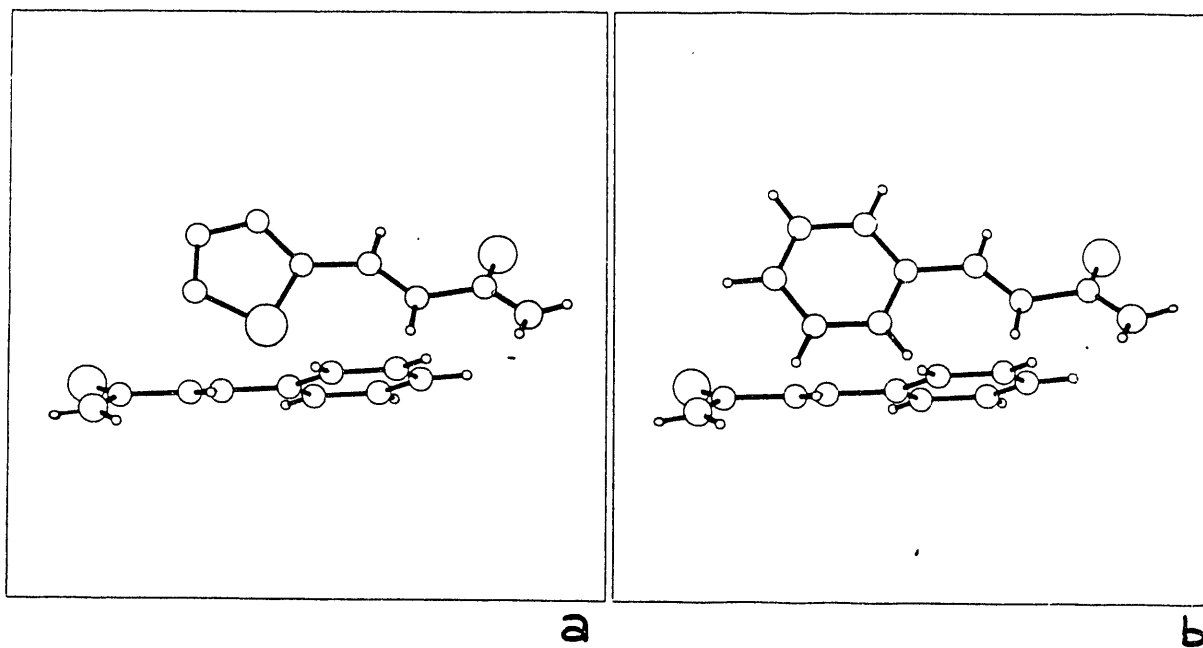


Figure 3: Herring-bone contacts between: (a) an absorbed 2-thienyl acrylamide molecule and a cinnamamide molecule; (b) two cinnamamide molecules.

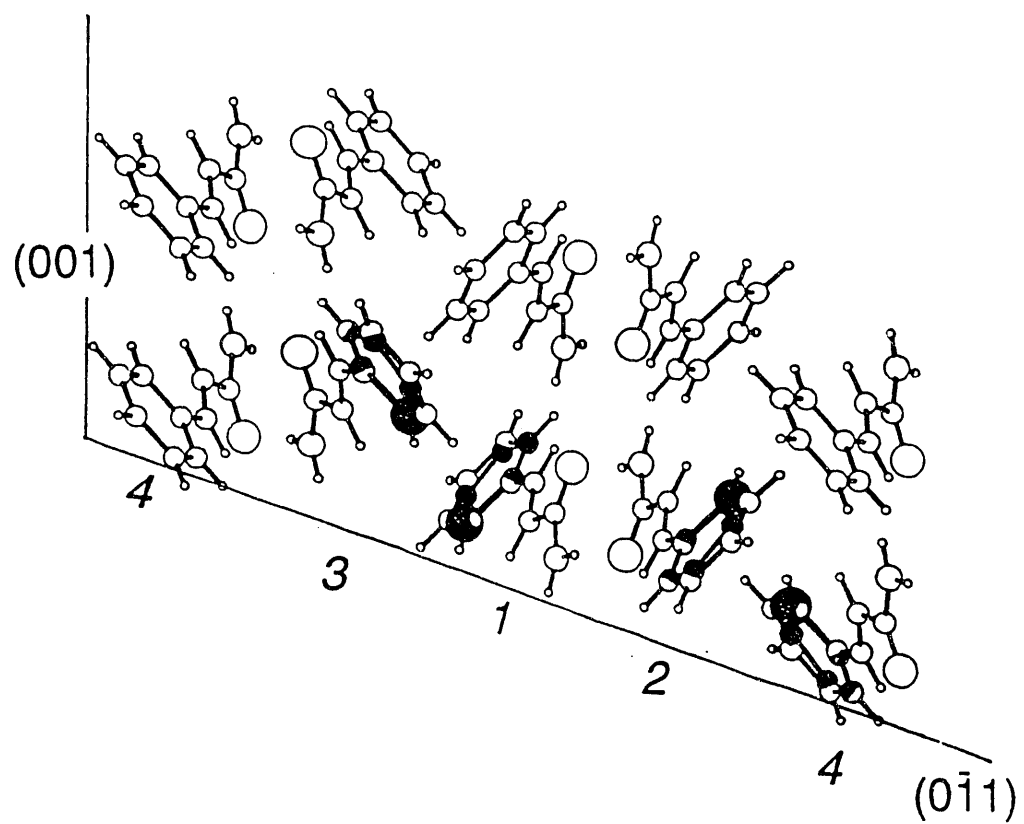


Figure 4: Packing arrangement of cinnamamide at the $(0\bar{1}1)$ face, showing the four different surface sites. The filled atoms are those of 2-thienyl rings in the positions they would assume were they to replace cinnamamide molecules.

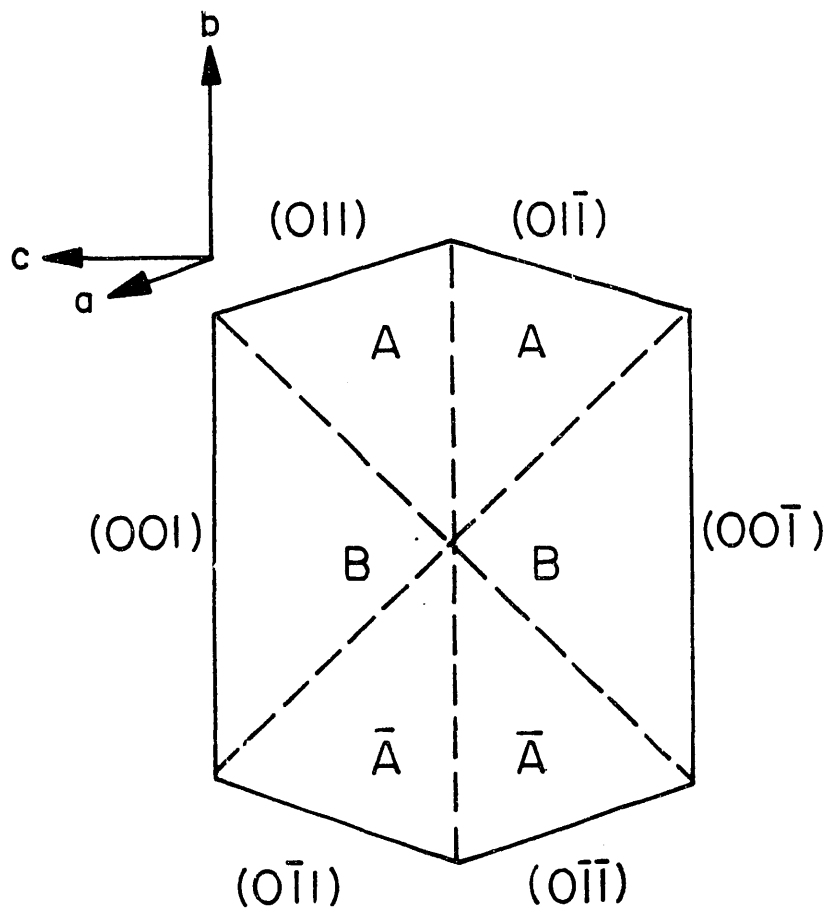


Figure 5: Morphological representation of a cinnamamide crystal, with sectors of reduced symmetry.

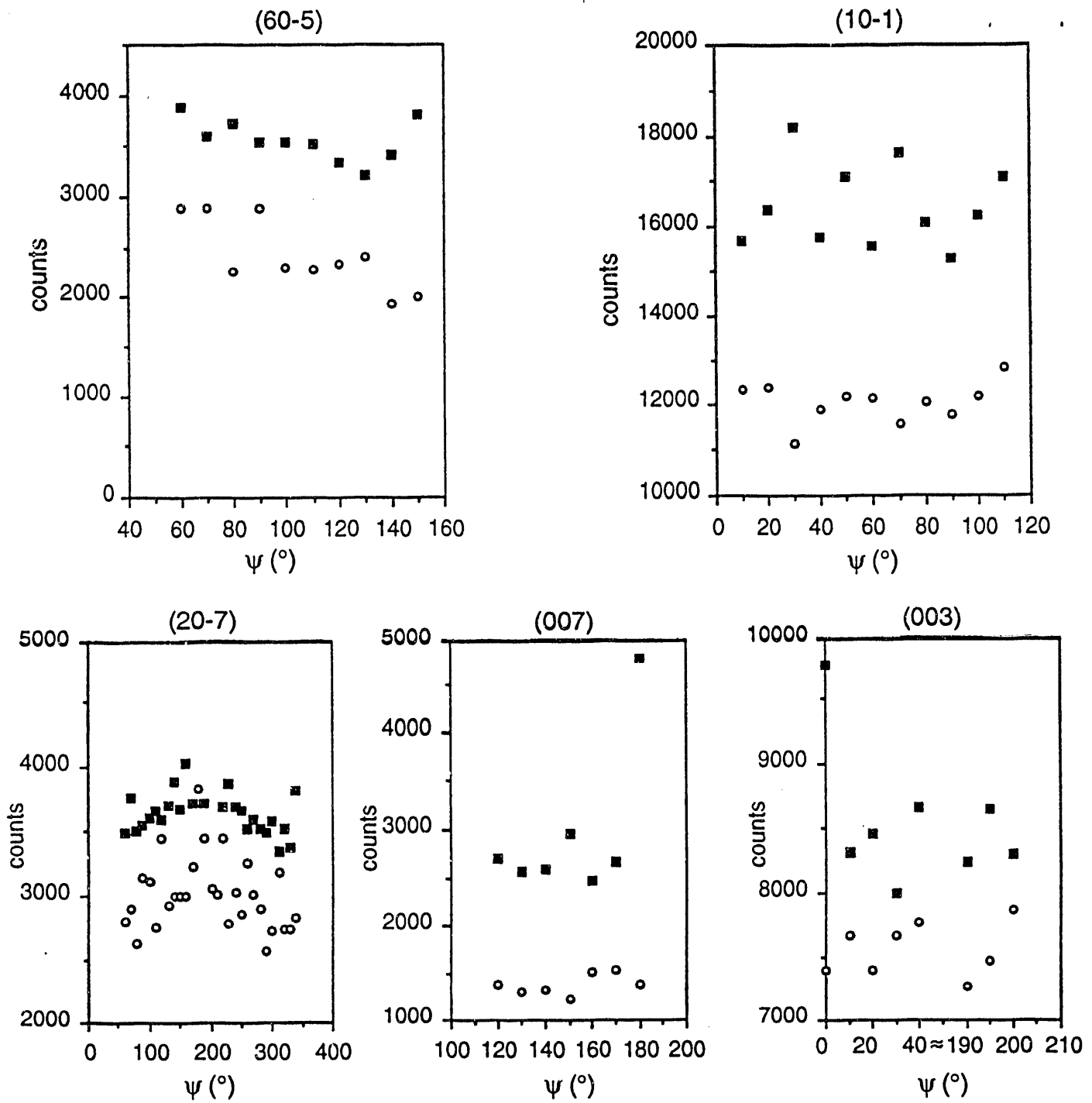


Figure 6 X-ray diffraction scans about the d^* (hkl) vector (ψ scan) of the $(60\bar{5})$, $(10\bar{1})$ and $(20\bar{7})$ reflections of sector $\bar{A}(0\bar{1}1)$ and of the (007) and (003) reflection of sector $A(011)$, showing integrated intensities (■) and background (○) for all measurable values of ψ . At some points along the ψ scans very high intensities were recorded, arising from multiple X-ray diffraction. These points are not indicated.

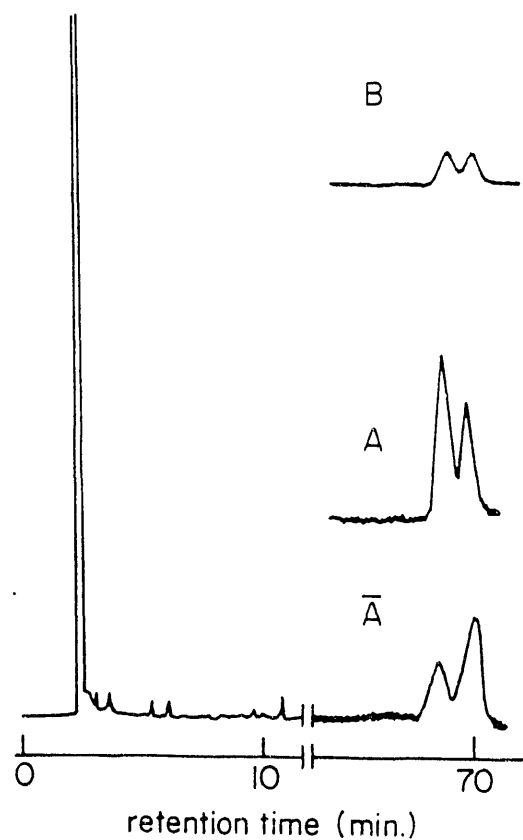


Figure 7: Gas chromatogram of the O-iPr-N-TFA derivatives of compounds *4a* and *4b* of sectors A, \bar{A} and B. The thiophene ring was reduced to an n-butylgroup (Chirasil-L-valine capillary column.)

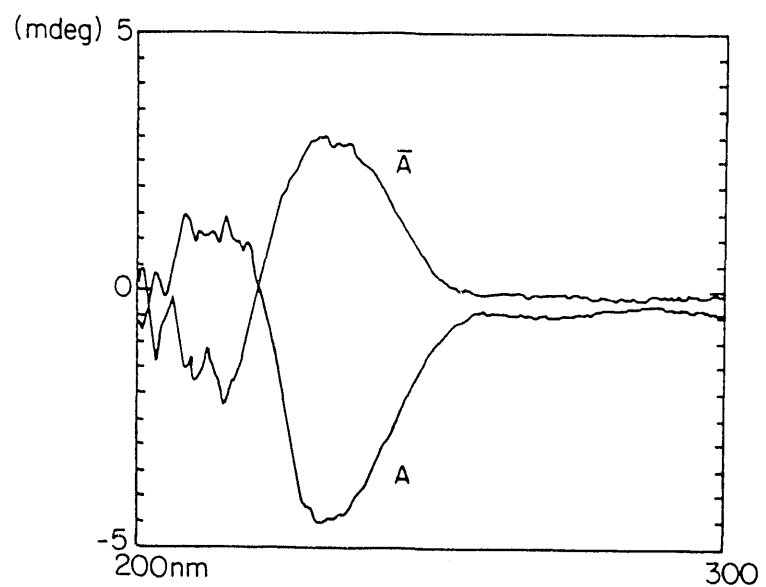


Figure 8: Circular dichroism spectra of photodimers *4a* and *4b* obtained from sectors A and \bar{A} , respectively.

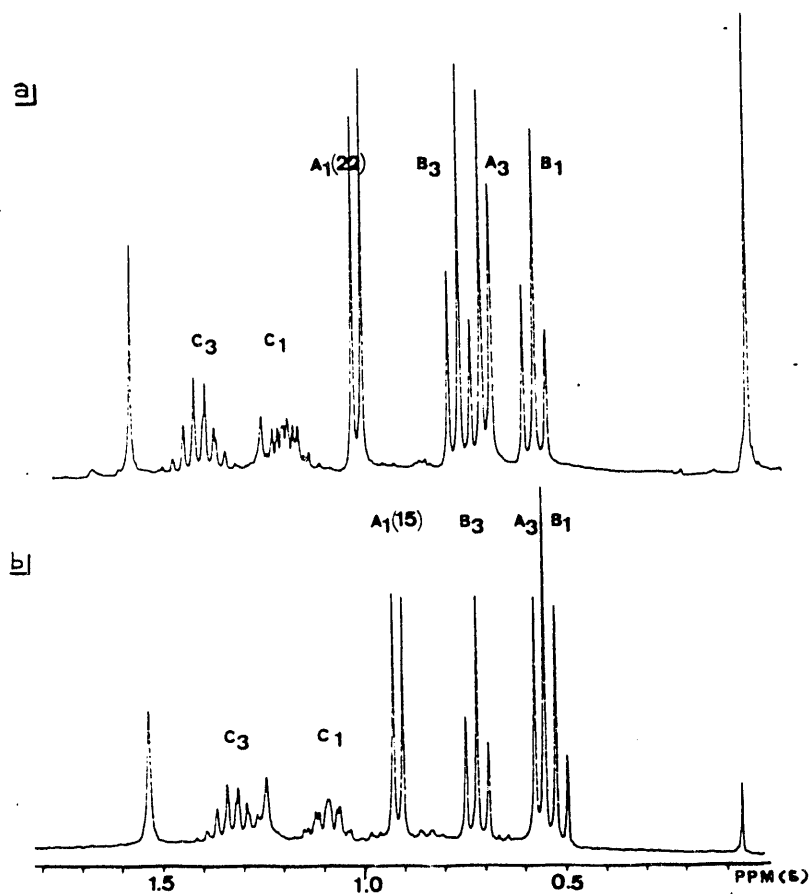


Figure 9: NMR spectrum of the methyl regions of:

(a) The di S-(+)-sec-butyl ester of **6**. By esterification the compound lost its center of inversion and became chiral of absolute configuration 1S,2R,3R,4S.

(b) The corresponding diester of **5**. This compound also has absolute configuration 1S,2R,3R,4S. The doublets at 1.01 and 0.92 ppm respectively, belong to methyl group A of the sec-butyl ester at C1, which has absolute configuration S.

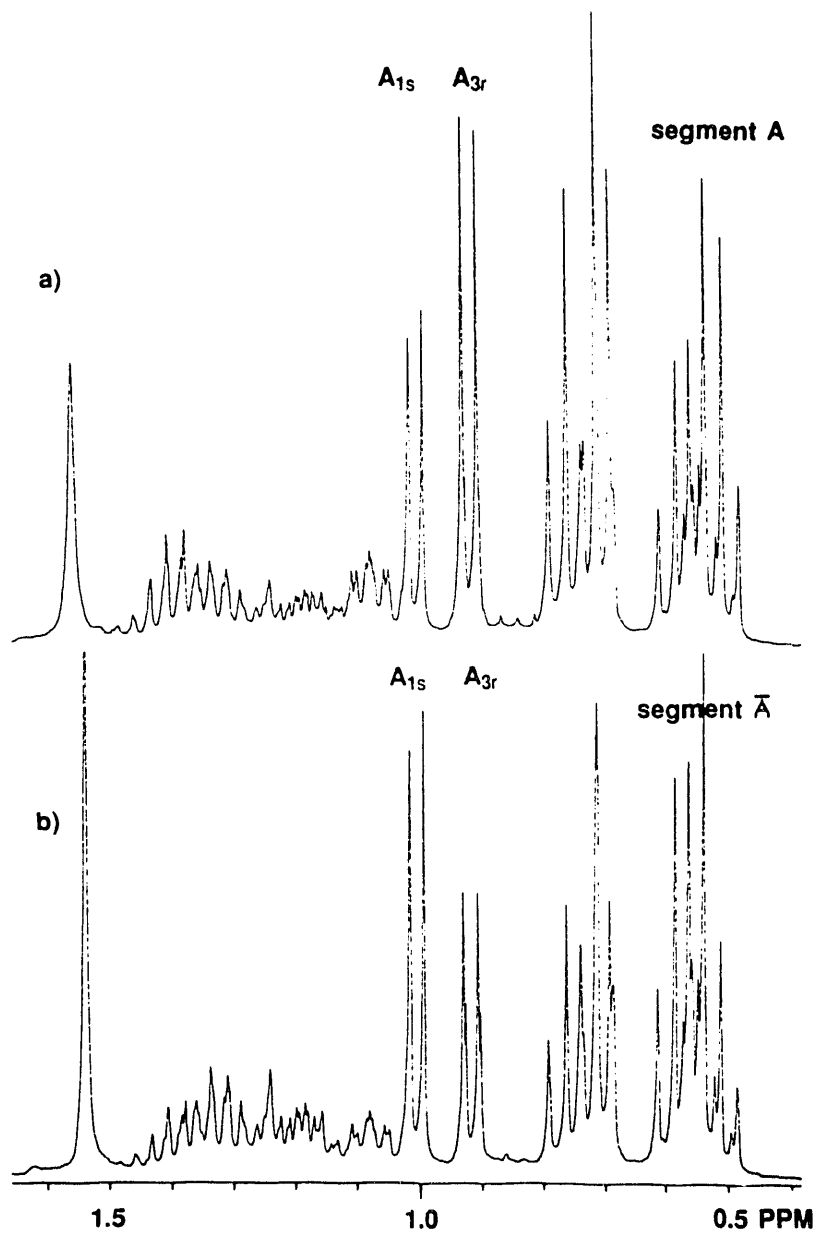


Figure 10: NMR spectrum of the methyl region of
 (a) The S-(+)-sec-butyl diester mixture of the material isolated from an *A* sector, which consists of 90% heterodimer **4**. The ratio of doublet $A_1:A_3$ is 4:6, meaning that the diastereomer in excess is 1*R*,2*S*,3*R*,4*R*, **4a**.
 (b) The corresponding diester of the material isolated from an \bar{A} sector, which also consists of 90% heterodimer **4**. In this case the ratio of doublet $A_1:A_3$ is 6:4, meaning that the diastereomer in excess is 1*S*,2*R*,3*S*,4*S*, **4b**.

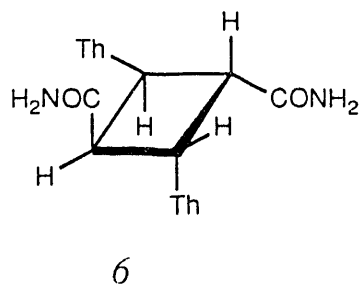
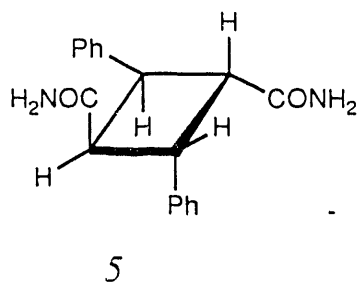
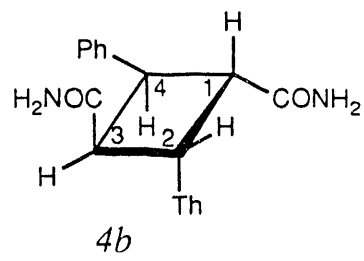
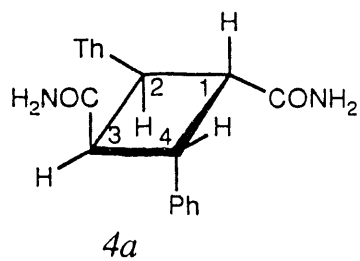
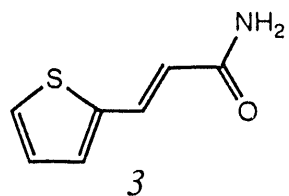
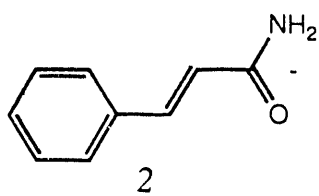


Table 1

X-RAY INTENSITY MEASUREMENTS AND CRYSTAL STRUCTURE REFINEMENT
OF PURE MATERIALS.

	E-cinnamamide	E-2-thienylacrylamide
(a) Crystal Data		
Formula	C ₉ H ₉ NO	C ₇ H ₇ NOS
Spacegroup	<i>P</i> 21/ <i>c</i>	<i>Pbca</i>
<i>a</i> (Å)	9.476(1)	19.2728(2)
<i>b</i>	5.0712(6)	8.4191(6)
<i>c</i>	15.625(1)	8.8989(1)
α (°)	90	90
β	92.721(1)	90
γ	90	90
V(Å) ³	751.3	1443.9
<i>z</i>	4	4
Temperature (°K)	100	100
X-radiation	CuKα (1.5418 Å)	CuKα (1.5418 Å)
crystal size 10 ⁻¹ mm ⁻³	3 x 3 x 3	3 x 3 x 3
No. of reflections measured	2345	1342
No. of independent reflections	1056	1001
<i>R_m</i> (<i>F</i> ²)**	0.073	0.014
(b) Crystal Structure Refinement		
No. of parameters refined	137	124
<i>R</i> (<i>F</i>)	0.034	0.059
<i>R_w</i> (<i>F</i>)	0.046	0.066

** $R_m(F^2) = \frac{\sum |F^2 - F_i^2|}{\sum F_i^2}$ where F^2 is the average of the set of observed symmetry-related structure factors and F_i^2 is the *i*th individual observed structure factor.

Table 2

CRYSTALLOGRAPHIC DATA AND NEUTRON DIFFRACTION MEASUREMENTS*.

Crystal sample	E-cinnamamide pure	Affected cinnamamide P1-segment
principal faces	{100},{001},{010},{012}	{101},{001},{011}
dimensions (mm)	2.8 x 2.0 x 1.1	1.7 x 1.9 x 2.2
volume (mm ³)	6.30	4.27
absorption coefficient (μ.cm ⁻¹)	1.97	0.55
Diffraction measurements		
Temperature (°K)	100.0(5)	200.0(5)
wavelength (Å)	1.0353	1.15930(12)
scan method	θ/2θ	θ/2θ
scan lengths (0°<2θ<55°)	3.2	3.0
in 2θ (55°<2θ<111°)	1.79 + 4.83 tan θ	1.45 + 2.941 tan θ
reciprocal lattice sector	(h, -k, ±l)	(-h, ±k, ±l)
sinθ/λ limit (Å ⁻¹)	0.68	0.71
No. of observations		
total	3528	5060
independent (N)	3276	4618

*Cell dimensions *a*, *b*, *c*, α , β , γ are given in Table 3.

Table 3

Cell dimensions of Cinnamamide pure and Cinnamamide-2-thienylacrylamide crystal segments

Crystal	Radiation	Temp. (°K)	a(Å)	b(Å)	c(Å)	α(°)	β(°)	γ(°)
Pure	x-ray	100	9.476(1)	5.0712(6)	15.652(1)	89.999(2)	92.721(2)	90.008(2)
Pure	neutron	100	9.471(3)	5.0729(3)	15.635(5)	90	92.71	90
Affected A(011)	x-ray	100	9.454(1)	5.0686(2)	15.682(5)	90.018(6)	92.697(5)	89.871(4)
Affected $\bar{A}(0\bar{1}1)$	x-ray	100	9.459(1)	5.0685(2)	15.688(2)	89.969(20)	92.749(30)	90.113(4)
Affected A(01 $\bar{1}$)	neutron	200	9.496(2)	5.0742(8)	15.821(1)	89.980(1)	93.18(6)	90.114(2)
Affected B(001)	x-ray	100	9.462(2)	5.0704(2)	15.674(3)	89.998(2)	92.703(2)	90.005(2)

Table 4

Refined Occupancies of Guest Thienylacrylamide Molecules at the four Molecular Sites 1 (x,y,z), 2 (-x,-y,-z), 3 (-x,1/2+y,1/2-z), 4 (x,1/2-y,1/2+z) in the Three P1 segments $A(01\bar{1})$, $A(011)$, $\bar{A}(0\bar{1}\bar{1})$.

site	$A(01\bar{1})$	site	$A(011)$	site	$\bar{A}(0\bar{1}\bar{1})$	Average
1	0.000	3	0.022(2)	2	0.025(2)	0.016
2	0.144(10)	4	0.139(2)	1	0.155(2)	0.146
3	0.017(10)	2	0.106(2)	3	0.074(3)	0.066
4	0.088(10)	1	0.046(2)	4	0.055(2)	0.063

SUPPLEMENTARY MATERIAL

X-RAY DIFFRACTION DATA

E-CINNAMAMIDE AT A TEMPERATURE OF 100°K.

Fractional Atomic Coordinates ($\times 10^4$) and Displacement Parameters ($\text{\AA}^2 \times 10^3$).

atom	x/a	y/b	z/c	$U_{eq/iso}$
O(1)	1540(1)	2036(2)	5419(1)	27
N(2)	1123(1)	-2298(2)	5621(1)	22
C(3)	1948(1)	-170(3)	5671(1)	20
C(4)	3390(1)	-563(3)	6062(1)	21
C(5)	4377(1)	1279(3)	6004(1)	20
C(6)	5837(1)	1235(3)	6367(1)	20
C(7)	6304(1)	-656(3)	6972(1)	22
C(8)	7675(1)	-628(3)	7305(1)	25
C(9)	8616(1)	1284(3)	7048(1)	27
C(10)	8171(2)	3170(3)	6460(1)	28
C(11)	6788(1)	3149(3)	6127(1)	24
H(1)	4122(18)	2883(35)	5702(10)	32
H(2)	5669(18)	-2020(31)	7140(10)	22
H(3)	8001(19)	-1939(34)	7727(11)	39
H(4)	3552(17)	-2258(32)	6348(10)	29
H(5)	9568(20)	1288(34)	7309(12)	36
H(6)	8786(18)	4508(34)	6284(10)	31
H(7)	6476(16)	4473(32)	5726(11)	25
H(8)	1452(17)	-3901(39)	5736(11)	32
H(9)	332(21)	-2104(28)	5337(11)	19

where $U_{eq} = (U_{11} + U_{22} + U_{33})/3$

X-RAY DIFFRACTION DATA

2-THIENYLACRYLAMIDE AT A TEMPERATURE OF 100°K.

Fractional Atomic Coordinates ($\times 10^4$) and Displacement Parameters ($\text{\AA}^2 \times 10^3$)

atom	x/a	y/b	z/c	$U_{\text{eq/iso}}$
S(1)	1398(1)	1373(1)	2148(1)	31
N(2)	-52(1)	1267(3)	-3299(4)	29
O(3)	484(1)	-987(2)	-3421(3)	30
C(4)	359(1)	210(3)	-2696(4)	26
C(5)	672(2)	519(4)	-1120(4)	28
C(6)	1117(2)	-441(4)	-449(4)	28
C(7)	1456(2)	-251(3)	1089(3)	22
C(8)	1861(2)	-1277(5)	1912(5)	27
C(9)	2094(2)	-775(4)	3358(4)	32
C(10)	1879(2)	677(4)	3674(4)	34
H(1)	563(16)	1520(37)	-665(37)	22
H(2)	1224(22)	-1445(45)	-974(53)	53
H(3)	1998(23)	1254(43)	4616(49)	46
H(4)	2412(27)	-1300(52)	4083(62)	67
H(5)	-218(23)	1116(47)	-4423(58)	60
H(6)	199(22)	-2949(50)	-2180(52)	77
H(7)	1992(19)	-2316(17)	1569(44)	60

where $U_{\text{eq}} = (U_{11} + U_{22} + U_{33})/3$

X-RAY DIFFRACTION DATA

CINNAMAMIDE/2-THIENYLACRYLAMIDE COMPOSITE MOLECULE AT A TEMPERATURE OF 100°K.

Fractional Atomic Coordinates ($\times 10^4$) and Displacement Parameters ($\text{\AA}^2 \times 10^3$)

atom	x/a	y/b	z/c	K	U_{eq}
O(1)	1539	2042	5423	1.000	31
N(2)	1111	-2292	5626	1.000	25
C(3)	1943	-167	5675	1.000	24
C(4)	3387	-569	6064	1.000	25
C(5)	4381	1268	6005	1.000	24
C(6)	5843	1215	6367	1.000	24
C(7)	6308	-680	6969	.922(2)	28
C(8)	7682	-660	7302	.922(2)	30
C(9)	8629	1248	7044	.922(2)	31
C(10)	8187	3138	6458	.922(2)	33
C(11)	6801	3125	6127	.922(2)	29
S(1)	6493	-799	7066	.078(2)	28
C(6')	5846	1431	6336	.078(2)	24
C(9')	8158	465	7057	.078(2)	31
C(10')	8211	2612	6517	.078(2)	33
C(11')	6916	3147	6120	.078(2)	29

where $U_{eq} = (U_{11} + U_{22} + U_{33})/3$

Since the composite molecule was refined as two rigid bodies the estimated standard deviations in x,y,z ($\times 10^4$) for cinnamamide and the thiophene ring are (1,2,1) and (6,8,4) respectively.

The atoms of the thiophene ring are marked with an asterisk'.

X-RAY DIFFRACTION DATA

CINNAMAMIDE/2-THIENYLACRYLAMIDE COMPOSITE MOLECULE AT A TEMPERATURE OF 100°K.

Fractional Atomic Coordinates ($\times 10^4$) and Displacement Parameters ($\text{\AA}^2 \times 10^3$)

atom	x/a	y/b	z/c	K	U_{iso}
H(12)	4128	2874	5704	1.000	36
H(13)	3545	-2266	6348	1.000	36
H(14)	5669	-2041	7137	.922(2)	40
H(15)	8006	-1973	7721	.922(2)	40
H(16)	9583	1226	7304	.922(2)	40
H(17)	8806	4473	6282	.922(2)	40
H(18)	6490	4451	5726	.922(2)	40
H(1')	1436	-3899	5740	1.000	33
H(2')	318	-2094	5342	1.000	36
H(16')	895	-208	7409	.078(2)	38
H(17')	908	3659	6477	.078(2)	38
H(18')	684	-4674	5717	.078(2)	38

Since the composite molecule was refined as two rigid bodies the estimated standard deviations in x,y,z ($\times 10^4$) for cinnamamide and the thiophene ring are (1,2,1) and (6,8,4) respectively.

The atoms of the thiophene ring are marked with an asterisk'.

NEUTRON DIFFRACTION DATA

E-CINNAMAMIDE AT A TEMPERATURE OF 100°K.

Atomic Positional Parameters of Pure Cinnamamide

Atom	x	y	z
C5	0.43838(5)	0.12898(11)	0.60021(3)
O1	0.15401(7)	0.20345(12)	0.54190(5)
N2	0.11172(4)	-0.23053(7)	0.56191(3)
C3	0.19497(5)	-0.01735(10)	0.56711(3)
C4	0.33911(5)	-0.05787(10)	0.60648(3)
C7	0.62978(5)	-0.06709(11)	0.69709(3)
C8	0.76805(6)	-0.06326(11)	0.73121(4)
C6	0.58352(5)	0.12261(11)	0.63690(3)
C9	0.86289(6)	0.12821(12)	0.70527(4)
C10	0.81808(6)	0.31821(12)	0.64612(4)
C11	0.67904(6)	0.31653(11)	0.61266(3)
H12	0.40830(14)	0.30524(27)	0.56371(9)
H13	0.36018(14)	-0.24276(27)	0.63977(10)
H14	0.55757(14)	-0.21717(29)	0.71815(9)
H15	0.80167(15)	-0.21003(32)	0.77861(10)
H16	0.97070(14)	0.12828(35)	0.73196(10)
H17	0.89076(15)	0.46935(33)	0.62602(11)
H18	0.64459(16)	0.46717(29)	0.56682(9)
HN1	0.01585(12)	-0.21503(25)	0.52920(8)
HN2	0.15179(14)	0.41368(23)	0.57182(9)

Thermal Parameters of Pure Cinnamamide (x10²)*

Atom	U ₁₁	U ₂₂	U ₃₃	U ₁₂	U ₁₃	U ₂₃
C5	1.16(2)	1.23(2)	1.66(2)	-0.08(2)	-0.27(2)	0.12(2)
O1	1.57(3)	0.92(2)	3.36(3)	0.08(2)	-1.00(2)	0.05(2)
N2	1.26(1)	1.11(2)	2.26(2)	-0.10(1)	-0.42(1)	0.10(1)
C3	1.12(2)	0.93(2)	1.83(2)	0.04(2)	-0.34(2)	-0.13(2)
C4	1.12(2)	1.14(2)	1.93(2)	0.02(2)	-0.35(2)	0.13(2)
C7	1.07(2)	1.55(2)	1.83(2)	-0.10(2)	-0.14(2)	0.37(2)
C8	1.13(2)	2.01(3)	2.24(2)	0.03(2)	-0.32(2)	0.37(2)
C6	1.07(2)	1.30(2)	1.35(2)	-0.11(2)	-0.08(2)	0.03(2)
C9	1.08(2)	2.24(3)	2.31(3)	-0.26(2)	-0.17(2)	-0.07(2)
C10	1.41(2)	2.11(3)	2.30(3)	-0.67(2)	-0.07(2)	0.15(2)
C11	1.52(2)	1.69(2)	1.86(2)	-0.48(2)	-0.13(2)	0.29(2)
H12	3.18(6)	2.76(6)	4.84(7)	-0.32(5)	-1.25(5)	1.55(6)
H13	2.96(6)	2.36(6)	5.83(3)	-0.15(5)	-1.37(6)	1.56(6)
H14	2.65(6)	3.36(7)	4.57(1)	-0.97(5)	-0.35(1)	1.71(6)
H15	2.95(6)	4.30(8)	5.09(8)	0.03(6)	-1.10(6)	2.18(7)
H16	1.93(5)	4.84(8)	5.22(8)	-0.37(6)	-1.00(5)	0.42(7)
H17	3.02(6)	4.34(8)	5.34(8)	-1.92(6)	-0.11(6)	1.23(7)
H18	3.78(7)	3.38(7)	4.42(7)	-0.77(6)	-0.80(6)	1.86(6)
HN1	2.09(5)	2.54(5)	4.02(6)	-0.16(4)	-1.06(4)	0.14(5)
HN2	2.69(6)	1.77(5)	4.71(7)	0.17(4)	-0.60(5)	0.54(5)

*Anisotropic thermal factors have the form:

$$\exp(-2\pi^2 \sum \sum h_i h_j a_j^* U_{ij})$$

0.7000(0) -0.06325(11) 0.73101743

HN2 0.151797173 0.52920(8)

END

**DATE
FILMED**

6 / 23 / 93

